Selective Production of Phenolic Aldehydes with Acetosolv Lignin Extracted from Corn Field Leftovers

Steffan Green

B.S. Chemical Engineering, University of Kansas, 2019

Submitted to the graduate degree program in Department of Chemical and Petroleum Engineering and the Graduate Faculty of the University of Kansas in partial fulfillment of the requirements for the degree of Master of Science.

Bala Subramaniam, Chairperson

Committee members

Laurence Weatherley

Kevin Leonard

Date defended: September 13, 2022

The Thesis Committee for Steffan Green certifies
that this is the approved version of the following thesis :

Selective Production of Phenolic Aldehydes with Acetosolv Lignin Extracted from Corn Field Leftovers

Bala Subramaniam, Chairperson

Date approved: December 2, 2022

Abstract

Annual U.S. production of lignocellulose from crop residues such as corn cobs and stover is nearly 400 million tons. Yet, it is a vastly underutilized resource. Global sustainability and biorefinery profitability will benefit from innovative technologies which valorize all lignocellulosic fractions to produce diverse chemical products alongside fuels. To this end, a valorization technology where phenolic aldehydes are selectively produced from lignin extracted from corn residues was devised. Lignin was extracted from lignocellulose in aqueous acetic acid and a sulfuric acid catalyst. Under agitated reflux conditions at 110 °C, corn residues were mildly hydrolyzed to cleave lignin-carbohydrate complexes (LCCs) and other inter-unit linkages. After separation from the cellulosic pulp and hemicellulose, the estimated yield of lignin is 14-17% by dry mass of corn residue. As revealed by 2D-NMR (^{1}H-^{13}C HSQC), lignin from corn cobs (CL) and corn stover (SL) are identical in the aromatic region and rich in phenyl-alkyl linkages. To produce phenolic aldehydes, the isolated lignins (SL and CL) were dissolved in a suitable protic solvent such as acetic acid then sprayed into a continuous phase of gaseous ozone at ambient temperature and pressure. The spray aerosolizes into fine droplets thus maximizing the gas-liquid interfacial area. This enhanced mass transfer area enables ozone to easily penetrate the droplets to preferentially cleave lignin's pendant C=C bonds according to the Criegee mechanism. Such spray ozonolysis occurs rapidly with a short residence of 5-8 s. Analysis with Gas Chromatography/Flame Ionization Detector (GC-FID) confirms the production of phenolic aldehydes, vanillin and *p*-hydroxybenzaldehyde (*p*HB). The cumulative yield of these products is ca. 10 wt.% of the initial lignin mass. Gel Permeation Chromatography (GPC) and HSQC of the remaining ozonized lignin reveals a largely intact macrostructure, suggesting that the ozonized lignin may be further valorized. Demonstration of these scalable concepts for lignin isolation and ozonolysis paves the way for further development towards potential commercialization with several value-added product streams.

Acknowledgements

To my advisor, Prof. Bala Subramaniam, for encouraging excellence and for his thoughtful mentorship from challenging me to develop creative solutions in sustainable processes to nurturing my professional development with many opportunities in industrial and academic circles.

To my project advisors, Dr. Thomas Binder and Dr. Erik Hagberg, for their infinite wisdom and unbridled counsel, especially on practical aspects of industry and biomass processing.

To Prof. Kevin Leonard and Prof. Laurence Weatherley, for serving on my committee and for their invaluable teachings and guidance throughout my studies.

To NSF's Partners For Innovation program (Grant No. 1919267) and KU's C&PE Department (SELF Scholarship and James & Catharine Combs Scholarship) for the funding and empowerment of these intellectual pursuits.

To the staff and collaborators of the CEBC for their unrivaled support in personal and academic endeavors through the challenges of the COVID-19 pandemic and beyond.

To my dear friends and colleagues, Dr. Hongda Zhu, Dr. Anoop Uchagawkar, Brandon Kinn, Brianna Farris, and Jane Wang for their fellowship and camaraderie.

To my loving father, mother, brother, and sister for whom I would not achieve without their support and devotion.

To myself.

Contents

1 Introduction and State of the Art **1**

1.1 Lignocellulose 1

1.1.1 Composition 2

1.1.2 Sources 3

1.2 Lignocellulose Pretreatment 4

1.2.1 Steam Explosion 5

1.2.2 Kraft Process 6

1.2.3 Sulfite Pulping 6

1.2.4 Organosolv Process 7

1.2.4.1 Acetosolv Process 7

1.3 Lignin as a Renewable Platform 8

1.3.1 Lignin Chemistry 8

1.3.1.1 Monolignols and Lignin Synthesis 8

1.3.1.2 Structural Motifs of Lignins 9

1.3.1.3 Lignin–Carbohydrate Complexes 12

1.3.2 Lignin Applications 13

1.3.2.1 Vanillin 14

1.3.2.2 Phenolic Resins 15

1.4 Lignin Valorization 16

1.4.1 Oxidative Pathway 16

1.4.1.1 Alkaline oxidation 17

1.4.1.2 Acidic oxidation 18

1.4.1.3 Oxidation in Ionic Liquids . . . 19
1.4.1.4 Non-Catalytic Oxidation with Ozone . . . 19
1.4.2 Reductive Pathway . . . 20
1.4.2.1 Mild Hydroprocessing . . . 20
1.4.2.2 Harsh Hydroprocessing . . . 21
1.4.2.3 Liquid-Phase Reforming . . . 21
1.4.2.4 Reductive Catalytic Fractionation . . . 22
1.4.3 Enzymatic Pathway . . . 23
1.5 Objective . . . 24

2 Acetosolv Extraction of Lignin from Corn Cobs 26
2.1 Background . . . 26
2.1.1 Physicochemical Mechanism . . . 27
2.2 Experimental . . . 28
2.2.1 Sourcing Corn Residues . . . 28
2.2.2 Developing a Large Lab-Scale Acetosolv Process . . . 28
2.2.3 Characterization of Extracted Lignins . . . 29
2.3 Results & Discussion . . . 30
2.3.1 Lignin Yield . . . 30
2.3.2 CHNO Elemental Analysis . . . 30
2.3.3 Molecular Weight Distribution . . . 31
2.3.4 Structural Analysis via HSQC NMR . . . 32
2.4 Conclusions . . . 33

3 Continuous Spray Ozonolysis of Acetosolv Lignin: Reactor Engineering Studies 34
3.1 Background . . . 34
3.1.1 Ozonolysis Reaction Mechanism . . . 35
3.1.2 Prior Work . . . 35

3.2 Experimental 36
3.2.1 Re-Engineering Lignin Spray Ozonolysis 36
3.2.2 Process Evaluation 37
3.2.3 Product Analysis and Characterization 37
3.3 Results & Discussion 39
3.3.1 Temporal Temperature and Ozone Consumption Profiles 39
3.3.2 Production of Phenolic Aldehydes 40
3.3.3 Ozone Utilization During Spray Ozonolysis 41
3.3.4 Ozonolysis Minimally Alters the Elemental Composition of Lignin 42
3.3.5 Molecular Weight Distribution of Ozonized Lignin 43
3.3.6 Functionality of Ozonized Lignin 43
3.4 Parametric Studies of Spray Ozonolysis Reactor 44
3.4.1 Effects of Flow Rates and Ozone Concentration 45
3.4.2 Solvent Effects 47
3.4.3 Combined Effect of Ozone Concentration and Gas Flow Rate 48
3.5 Conclusions 49

4 Future Prospects **51**
4.1 Improvements to Lignin Extraction 51
4.2 Improvements to Spray Ozonolysis of Lignin 52
4.3 Technoeconomic Assessment of a Modular Biorefinery 53

A Supplementary Information **65**
A.1 Abbreviations 65
A.2 Materials 65
A.2.1 Acetosolv Extraction 65
A.2.2 Spray Ozonolysis 66
A.3 Experimental Methods 66

A.3.1 Spray Ozonolysis of Lignin 66
A.3.2 Gas Chromatography/Flame Ionization Detector (GC/FID) & /Mass Spectroscopy (GC/MS) 67
A.3.3 Heteronuclear Single Quantum Coherence (HSQC) NMR 68
A.3.4 Fourier Transform Infrared Spectroscopy (FTIR) 68
A.3.5 Gel-Permeation Chromatography (GPC) 68
A.3.6 CHNO Elemental Analysis 69
A.4 Experimental Data 70
A.4.1 Blank Runs of Pure Solvent Sprayed into Ozone 70
A.5 Process and Equipment Photographs 72
A.6 Calculations for Elemental Analysis of Ozonized Cob Lignin 73

List of Figures

1.1 Rendering of the lignocellulose matrix containing cellulose (green fibers), hemicellulose (yellow strings), and lignin (red-orange clumps). Reprinted from Langan et al. (2014). 1

1.2 Xylan polymer bonded to ferulate esterase (Spiridon and Popa, 2008). 2

1.3 Summary of various lignocellulose pretreatments (Kumar and Sharma, 2017). . . . 4

1.4 Building block monolignols in the biosynthesis of lignin. 9

1.5 Generic structure of a grass lignin (Jasiukaitytė-Grojzdek et al., 2020). (red: β-O-4′; yellow: β-β' resinol; green: β-5′ phenylcoumaran; blue: ferulate esterase LCC) . 10

1.6 Common structural motifs found in grass-type lignins 11

1.7 Several known lignin-carbohydrate complexes (Tarasov et al., 2018). 12

1.8 Flavoring agents which may be extracted from lignin. 13

1.9 Pathways to synthesize vanillin from petrochemical feedstocks (Hocking, 1997). . 14

1.10 General scheme for the addition of formaldehyde to phenolic lignin to form lignin-based phenol-formaldehyde resins (Upton and Kasko, 2016). 15

2.1 Distribution of composition in corn residues. 26

2.2 Reaction scheme for the solvolytic hydrolysis of lignin during the acetosolv process (Jasiukaitytė-Grojzdek et al., 2020). 27

2.3 Diagram of acetosolv process developed for lab-scale fractionation of corn residues. 29

2.4 GPC spectrogram for lignin derived from corn stover (SL1) and corn cobs (CL1). . 31

2.5 Aromatic region of ^{1}H-^{13}C HSQC NMR spectrogram for stover lignin (SL1; left) and cob lignin (CL1; right). *p*CA: *p*-coumaric acid, FA: ferulic acid, G: guaiacyl, H: hydroxyphenyl. 32

3.1 Coumarates or ferulates in lignin can be converted to phenolic aldehydes using ozone. 34
3.2 General scheme for the ozonolysis of alkene bonds as described by Criegee (1975). 35
3.3 Schematic detailing the process of spray ozonolysis of lignin. 36
3.4 Phenolic aldehyde products, vanillin (24.14 min) and *p*HB (30.24 min), identified in the FID chromatogram of ozonized lignin (OZCL1) including monomer artifacts from extraction. 38
3.5 Temporal profiles recorded during continuous spray ozonolysis of CL1. Conditions: 1.0 wt.% CL1 at 4.5 LPH and 2.5 mol% O_3 at 3.0 SLPM. 39
3.6 Steady-state yields of phenolic aldehydes from continuous spray ozonolysis of lignin from corn residues. Conditions: 4.5 LPH of 1.0 wt.% lignin solution sprayed into 3.0 SLPM of 2.5 mol% O_3 at ambient temperature and pressure. 40
3.7 Ozone utilization during spray ozonolysis of various lignin sources where utilization is expressed as moles of produced aldehyde per moles of consumed ozone. . . 41
3.8 GPC spectra for untreated corn cob lignin (blue) and ozonized cob lignin (orange). 43
3.9 FTIR spectra of untreated (CL3; blue) and ozonized (OZCL3; red) cob lignin samples. 44
3.10 Investigations of the indicated parameters effect on the steady-state yields of phenolic aldehydes during spray ozonolysis of CL1. Conditions are listed in Table 3.2 except as noted. 46
3.11 Effect of various solvents on the steady-state yields of phenolic aldehydes during spray ozonolysis of SL3. Conditions are listed in Table 3.2, except solvent as indicated. 47
3.12 Combined effect of ozone concentration and total gas flow rate on the steady-state yields of phenolic aldehydes during spray ozonolysis of CL1. Ozone throughput was held constant at 75 SCCM for each run. Conditions are listed in Table 3.2, except as indicated. 48

3.13 Steady-state yields of phenolic aldehydes during spray ozonolysis when doubling lignin throughput in different gas phase dynamics at constant ozone throughput. Conditions are listed in Table 3.2, except as O_3 concentration and gas flow rate as indicated. 49

4.1 Twin-screw biomass extractor concept based on existing twin-screw granulation units. 51

A.1 External calibration curves for GC/FID quantification using purchased standards. . 67

A.2 Temporal temperature and ozone concentration profiles for spray ozonolysis experiment consisting of only **3:1 v/v AcOH:FmOH solution**. 70

A.3 Temporal temperature and ozone concentration profiles for spray ozonolysis experiment consisting of only **88% acetic acid**. 70

A.4 Temporal temperature and ozone concentration profiles for spray ozonolysis experiment consisting of only **88% formic acid**. 71

A.5 Temporal temperature and ozone concentration profiles for spray ozonolysis experiment consisting of only **water**. 71

A.6 Photo of acetosolv extraction setup including 4 L reactor with mixer and vacuum filtration. 72

A.7 Photo of spray ozonolysis setup including 6 L ozonolysis reactor and entrained vapor condenser. 72

List of Tables

1.1 Approximate cellulose, hemicellulose, and lignin contents of assorted lignocellulosic sources (Kumar and Sharma, 2017; Azadi et al., 2013). 3
1.2 Summary of technical lignins from common pretreatments. 5
1.3 Approximate composition of monolignol units in major biomass types (Tocco et al., 2021; Azadi et al., 2013). 8
1.4 Composition of structural motifs in various biomass sources (Wei Kit Chin et al., 2020; Azadi et al., 2013; Rinaldi et al., 2016). 11

2.1 Recoveries of cellulosic pulp and lignin from acetosolv processing of corn cobs. . 30
2.2 Elemental composition of acetosolv lignin samples extracted from corn cobs and stover. 31

3.1 Elemental composition of untreated and ozonized samples of lignin from corn cobs. 42
3.2 Baseline process conditions lignin ozonolysis. 45

Chapter 1

Introduction and State of the Art

1.1 Lignocellulose

The implementation of practically viable biorefineries, so called for their use of agricultural and lignocellulosic feedstocks, is a key component in the transition to a globally sustainable chemical industry. Present manufacturing and consumer demands of commodity chemicals require biorefineries to grow significantly and rapidly. Yet, current biorefining technologies struggle to attain economic viability without external subsidy due to the energy-intensive processing of agricultural feedstocks. New technologies must valorize all components of lignocellulose to attain commercial success. The largest fraction, cellulose, has been the driving force behind lignocellulose processing for thousands of years, while the lignin fraction offers very little practical value to date (Foroughi et al., 2021). Commercially viable technologies for converting lignin byproducts into value-added chemicals and materials will bolster the growth of biorefineries and green manufacturing.

Figure 1.1: Rendering of the lignocellulose matrix containing cellulose (green fibers), hemicellulose (yellow strings), and lignin (red-orange clumps). Reprinted from Langan et al. (2014).

1.1.1 Composition

Lignocellulose manifests as the fibrous material in plant cells which accounts for nearly all of the plant's mass, or biomass. The three-dimensional matrix of lignocellulose (Figure 1.1) is formed by the incorporation of lignin and hemicellulose as a protective barrier around the cellulose fibers (McMillan, 1994). Cellulose and hemicellulose are polysacharrides with varying degrees of homogeneity whereas lignin is heterogeneous aromatic polymer (Den et al., 2018; Tocco et al., 2021). The combination of these biopolymers is pivotal to the structural integrity of plants.

The most world's abundant biopolymer, cellulose, accounts for 40-50% of the lignocellulosic mass (Klemm et al., 1998). As a homogeneous polysaccharide, cellulose is composed of orderly glucose monomers chained by β-1,4-glycosidic bonds (Hendriks and Zeeman, 2009; Vogel, 2008). Strong hydrogen bonding between the uniformly linear chains affords a robust crystalline structure in all plant species (Tocco et al., 2021; Den et al., 2018). Textile makers have exploited cellulose's fibrous and crystalline properties for thousands of years (Klemm et al., 1998; Foroughi et al., 2021).

Hemicellulose is broadly comprised of branched polysaccharides which makes up for 30-45% of the biomass. (Dhepe and Sahu, 2010; Tocco et al., 2021; Vogel, 2008). In contrast to cellulose, hemicellulose is far more heterogeneous and less abundant (Spiridon and Popa, 2008). Hemicellulose often takes the form of hexosan and pentosan sugars including xylan, mannan, glucan, and arabinan monosaccharides interlinked by glycosidic bonds (Figure 1.2) (Dhepe and Sahu, 2010; Saha, 2003). Hydrogen-bonding is limited due to a notable absence of the C_6-hydroxyl in addition to other carboxyl or acetyl groups (McMillan, 1994; Spiridon and Popa, 2008). In turn, hemicellulose is more amenable to acid hydrolysis than cellulose (Saha, 2003; Tocco et al., 2021).

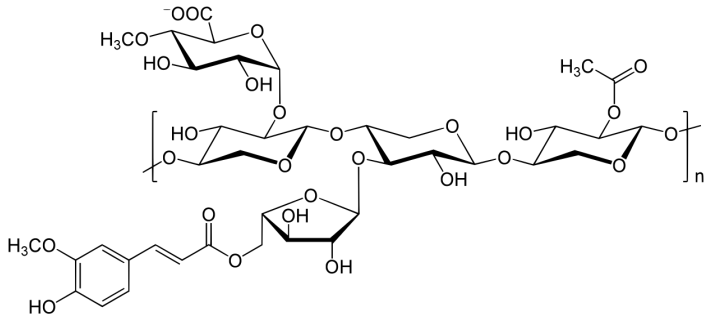

Figure 1.2: Xylan polymer bonded to ferulate esterase (Spiridon and Popa, 2008).

Lignin, the primary component of the plant's structural integrity and water management, accounts for the remaining 15-30% of dry biomass. Lignin is a heterogeneous biopolymer of phenylpropanoids bound by various aryl and ether linkages (Lora, 2008). During synthesis, reactive propyl side-chains combine with unsubstituted aromatic regions resulting in a highly cross-linked and amorphous 3D polymer. Lignin's commercial utility is notably challenged by its uniquely complex structure and water insolubility (Lora, 2008).

Discussed in further detail in Section 1.3.1, a variety of structural motifs may be identified in the seemingly random macrostructure of native lignins. Extraction of lignin from biomass may induce side reactions giving rise to unique forms of lignin known as technical lignins. Natural variation in growing conditions and plant function further diversifies the compositions of lignin. For these reasons, *lignin* encompasses a diverse collection of biopolymers. The importance of designating its source and extraction cannot be understated.

1.1.2 Sources

The ubiquity of woody plants leads to an abundant variety of potentially viable feedstocks for extracting cellulose and lignin. For example, trees are the main source of lignocellulose for the extensive history of the paper and pulping industry. Lignocellulose from trees is often categorized into either softwood or hardwood pulps. Paper and pulping mills traditionally use softwoods such

Table 1.1: Approximate cellulose, hemicellulose, and lignin contents of assorted lignocellulosic sources (Kumar and Sharma, 2017; Azadi et al., 2013).

Source	**Cellulose (wt.%)**	**Hemicellulose (wt.%)**	**Lignin (wt.%)**
Softwood	45-50	25-35	25-35
Hardwood	40-55	24-40	18-25
Corn stover	38	26	19
Corn cobs	45	35	15
Miscanthus	43-57	21-24	19-24
Wheat straw	29-45	26-32	16-22
Sugarcane bagasse	42-49	25-31	19-20
Sweet sorghum	45	27	21

as pine and spruce or eucalyptus, a hardwood (Ten and Vermerris, 2015).

Besides trees, other herbaceous or grass-like woody plants are processed for their lignocellulose. These types often include annual flowering plants such as sorghum and switchgrass or annual crops such as corn, sugarcane, and wheat (Ten and Vermerris, 2015). Lignocellulose from grasses and annual crops are distinct from hardwoods and softwoods, including additional differentiation even amongst the assorted crop species. As inferred from Table 1.1, there are variations even within softwoods, hardwoods, and grasses.

Annual crops and field residues present an intriguing opportunity as feedstocks for renewable chemicals and materials due to their low cost and favorable environmental impact. In contrast to the pulping industry, biorefineries frequently use grass-types in addition to poplar and willow hardwoods (Kumar and Sharma, 2017). Investigations of other agricultural residues including corn, wheat, sorghum, sugarcane, and bamboo are ongoing. However, many of these emerging feedstocks pose challenging economics unless more than cellulose is valorized (Kautto et al., 2014).

1.2 Lignocellulose Pretreatment

Fractionation of lignocellulose is commonly known as either *delignification* or *lignocellulose pretreatment*. While both terms indicate a separation of sorts, their usage highlights different motivations. When the treatment intends to preferentially isolate the cellulose fraction (i.e., cellulose-centric), it is considered to be a delignification process. In contrast, the ambiguity of lignocellu-

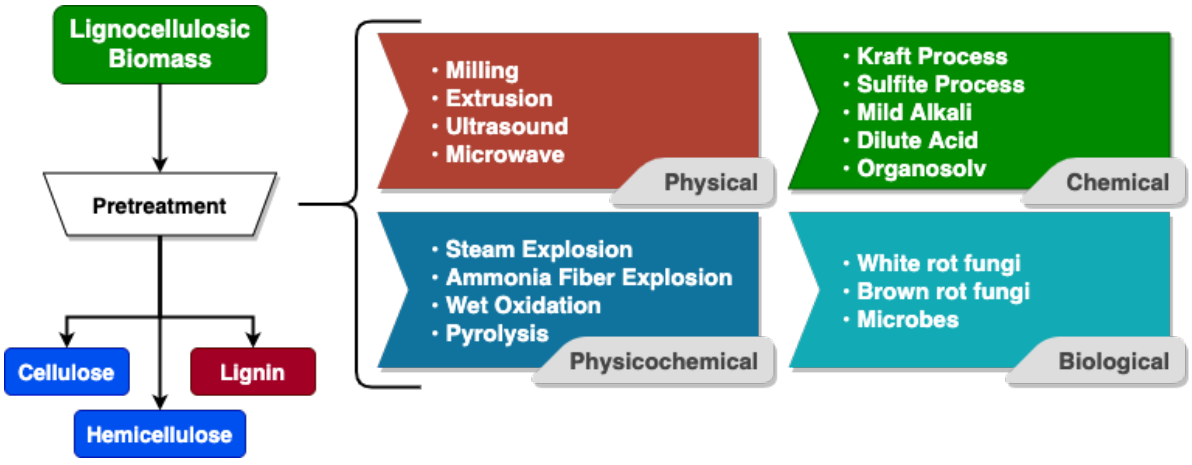

Figure 1.3: Summary of various lignocellulose pretreatments (Kumar and Sharma, 2017).

lose pretreatment could refer to a process that is cellulose-centric or lignin-centric or both. Figure 1.3 summarizes the categories of pretreatments which range from physical to chemical including physicochemical and biological routes (Kumar and Sharma, 2017).

Historically, delignification has referred to prominent cellulose industries including paper and pulping. Such industries employ the Kraft process or sulfite pulping to recover cellulosic pulp from woody biomass without regard for hemicellulose or lignin (Wild et al., 2014). Lignocellulose pretreatments may be used in other industries (e.g., biorefineries) that prefer clean and resource-efficient fractionation such as steam explosion or organosolv. The above mentioned technologies, the Kraft process, sulfite pulping, steam explosion, and the organosolv process, will be detailed below. Key commercial producers and properties of each process are supplied in Table 1.2.

Table 1.2: Summary of technical lignins from common pretreatments.

Technical Lignin	**Commercial Producer**	**Chemistry**	**Sulfur Content**	**Purity**
Steam explosion	Cambi (pilot)	mild acidic	free	high
Kraft	Domtar	alkaline	moderate	moderate
Lignosulfonate	Borregaard	alkaline/acidic	high	low
Organosolv	CIMV (pilot)	acidic	free	high

1.2.1 Steam Explosion

During steam explosion, biomass is rapidly blasted with high-pressure (0.7-4.8 MPa) saturated steam. Between blasts, the system is abruptly depressurized to atmosphere while remaining at high temperatures of 160-260 ºC (Kumar et al., 2009). Forceful decompression and rapid evaporation of water causes the biomass to explosively fragment (Brodin et al., 2017; McMillan, 1994). During fragmentation, ether bonds are physically broken in addition to the formation of acids from acetyls. These acids are thought to be responsible for subsequent hydrolysis to the biomass (Jacquet et al., 2015). The value of steam explosion lies in its ability to isolate cellulose and lignin close to their native states, avoiding major structural damage or modification. (Brodin et al., 2017).

1.2.2 Kraft Process

The Kraft process is the most common of chemical treatments. Popularized by the paper and pulping industry, Kraft pulp constitutes nearly 90% of all pulps due to its versatility and efficiency (Schutyser et al., 2018). Through a series of steps including alkali cooking, washing, and bleaching, NaOH and Na_2S solutions break down lignin (Bajwa et al., 2019). At 160-180 ºC and pH > 12, phenolic groups ionize and the lignin solubilizes into a black liquor (Kumar and Sharma, 2017). After cooking, cellulose remains as pulp while the black liquor contains hemicellulose, lignin residues, and inorganic extracts. To recover Kraft lignin, black liquor must undergo further purification and precipitation, demonstrated by Innventia's LignoBoost process (Bajwa et al., 2019). Sulfur content reaches 1-2% in Kraft lignins due to the added thiol functionality (Ahvazi et al., 2016). Companies such as MeadWestvaco in the U.S. and Canada-based Domtar produce a majority of industrial Kraft lignins (Mandlekar et al., 2018). Economics of the Kraft process and its superior cellulose pulp make it attractive, but its environmental impact is a cause for concern.

1.2.3 Sulfite Pulping

Sulfite pulping is another chemical delignification strategy made popular by the paper and pulping industries. The process begins with a 4 hour soak at 130-160 ºC in sulfur dioxide and calcium, sodium, or magnesium solution (Schutyser et al., 2018). Depolymerization is initiated via ether breakage by sulfite or bisulfite ions. Roughly 5% of the lignin is displaced by sulfur as a result of sulfonating the α-carbon of the propyl side-chains (Ahvazi et al., 2016). Some carbohydrates are retained in the sulfite liquor thus necessitating purification similar to black liquor (Lora, 2008).

Unlike Kraft lignin, sulfite-based lignins are the most commercially viable of all technical lignins. Functionalization with low pKa sulfonate groups (pKa ≤ 2) makes lignosulfonates one of the only water-soluble technical lignins (Ahvazi et al., 2016). Their unique properties created a sizeable market at ca. 800,000 MT annually, making them the most abundant technical lignin (Bajwa et al., 2019). Several companies are known to produce lignosulfonates including Tembec in Canada and Norway's Børregaard (Mandlekar et al., 2018).

1.2.4 Organosolv Process

In contrast to Kraft or sulfite pulping, organosolv processing utilizes the whole biomass efficiently while maintaining minimal alterations to the lignocellulose fractions. The primary mechanism is to solubilize the lignin and hemicellulose away from the cellulose fibers using aqueous organic acids, alcohols, or other organic solvents (Kumar et al., 2009). Reaction temperatures are solvent-dependent but typically moderate between 100-210 ºC (Schutyser et al., 2018; Pan et al., 2006). Effective variations of organosolv include acetic acid (Pinheiro et al., 2017), ethanol (Zijlstra et al., 2019), formic acid (Li et al., 2012), methyl isobutyl ketone (Teng et al., 2016), γ-valerolactone (Shuai et al., 2016), and more (Wei Kit Chin et al., 2020).

Organic solvents are known to hydrolyze the acid-labile ether linkages between lignin, hemicellulose, and cellulose (Jasiukaitytė-Grojzdek et al., 2020). Similar to the sulfur-based methods, lignin is solubilized by the solvolytic degradation at the α-position. Under organosolv conditions, this position is also prone to condensation reactions, rendering the lignin recalcitrant (Ahvazi et al., 2016). Organosolv processes can afford highly crystalline cellulose and hemicellulose in addition to sulfur-free lignin with minor carbohydrate carryover (Ragauskas et al., 2014; Xu et al., 2020).

Organosolv pretreatment is preferred for its effective delignification using environmentally benign chemicals with minimal effect on the lignin (Li et al., 2012; Vila et al., 2003). Compared to other pulping methods, the associated operating costs of organosolv process are often higher (Kautto et al., 2014; Budzinski and Nitzsche, 2016; Vila et al., 2003). However, the excellent quality of the fractions may lower downstream processing costs and lead to high-value downstream products (Li et al., 2012). Yet, organosolv fractions of lignin and hemicellulose require practical valorization strategies for the organosolv process to become commercially viable.

1.2.4.1 Acetosolv Process

A promising organosolv variation, the acetosolv process, aqueous acetic acid (near 70% w/w) at ca. 200 ºC (Li et al., 2012). Energy costs can be substantially decreased by reducing the reaction temperature to 110 ºC with the addition of H_2SO_4 catalyst. Utilizing an easily recoverable solvent

that is inexpensive and food-grade makes the acetosolv process particularly attractive. Although fundamentally similar, acetosolv may be more advantageous for cellulosic ethanol production compared to other organosolv variations. Acetic acid is known to minimize the formation of chemical species which inhibit enzymatic hydrolysis during ethanol production (Li et al., 2012).

In the past decades, several studies have investigated the acetosolv process for non-traditional biomass. Pinheiro et al. (2017) isolated lignin from sugarcane bagasse, Li et al. (2012) fractionated bamboo, and Ligero et al. extracted lignin from Miscanthus (2005) and eucalyptus saplings (2008).

1.3 Lignin as a Renewable Platform

The annual global production of lignin is projected to reach nearly 300 million MT by 2030 (Bajwa et al., 2019). This alone should incentivize commercial applications of lignin. Yet, despite being the largest source of renewable aromatics, only 2% of lignin is used commercially outside of energy generation (Lora, 2008). The properties of lignin that are essential to plants, protection, UV resistance, hydrophobicity, and chemical stability, pose challenges to chemically valorize lignin.

Table 1.3: Approximate composition of monolignol units in major biomass types (Tocco et al., 2021; Azadi et al., 2013).

Source	H units (%)	G units (%)	S units (%)
Softwoods	trace	90-95	5-10
Hardwoods	trace	50	50
Grasses	5	70	25

1.3.1 Lignin Chemistry

1.3.1.1 Monolignols and Lignin Synthesis

Plants biosynthesize lignin through the radical polymerization of three key precursors, or monolignols, *p*-coumaryl, coniferyl, and sinapyl alcohols (Bajwa et al., 2019). These monolignols, shown in Figure 1.4, share a similar structure of a phenolic region and propyl side-chain. In lignin, the monolignols are denoted as hydroxyphenyl (H), guiacyl (G), and syringyl (S) units,

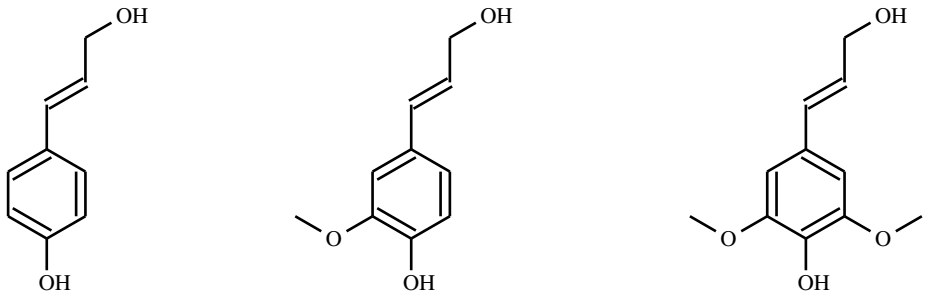

(a) *p*-coumaryl alcohol (b) coniferyl alcohol (c) sinapic alcohol

Figure 1.4: Building block monolignols in the biosynthesis of lignin.

respectively. Lignin's characteristic cross-linked nature is caused by oxidative coupling of the monolignols at various molecular positions (Boerjan et al., 2003). Polymerization of the unsaturated side-chain or radical delocalization may lead to additional functionality including ethers, esters, phenolic and free hydroxyls, methoxyls, carbonyls, and carboxyls (Bajwa et al., 2019; Ten and Vermerris, 2015). Thus, lignin is often described as an amorphous polymer of phenylpropanoids.

As previously noted, structures of native lignin have a high degree of variability. Typical compositions can be found in Table 1.3. In general, softwood lignins almost entirely contain G-units with some S-units while hardwood lignins consist of equal quantities of G- and S-units and trace H-units. Grass lignins are more balanced, comparatively, but G-units still dominate (Tocco et al., 2021). An example of a generic grass-type lignin structure is provided in Figure 1.5.

An in-depth discussion of the biosynthetic pathway is out of scope for this work. The reader is referred to other works, Boerjan et al. (2003), Vogel (2008), and Vanholme et al. (2010, 2019).

1.3.1.2 Structural Motifs of Lignins

Although lignin can seem an amalgam of randomly linked monolignols, a common pattern of linkages can be identified as structural motifs. Because plant source, biosynthetic pathway, and extraction process heavily influence the abundance of motifs, this discussion is aimed at native lignins which may also inform the structure of technical lignins. Figure 1.6 illustrates various motifs found in grass lignins. Typical proportions of notable motifs for hardwoods, softwoods, and grasses are provided in Table 1.4.

Nearly two-thirds of lignin consists of alkyl-aryl ether linkages while ether or $C-C$ linkages

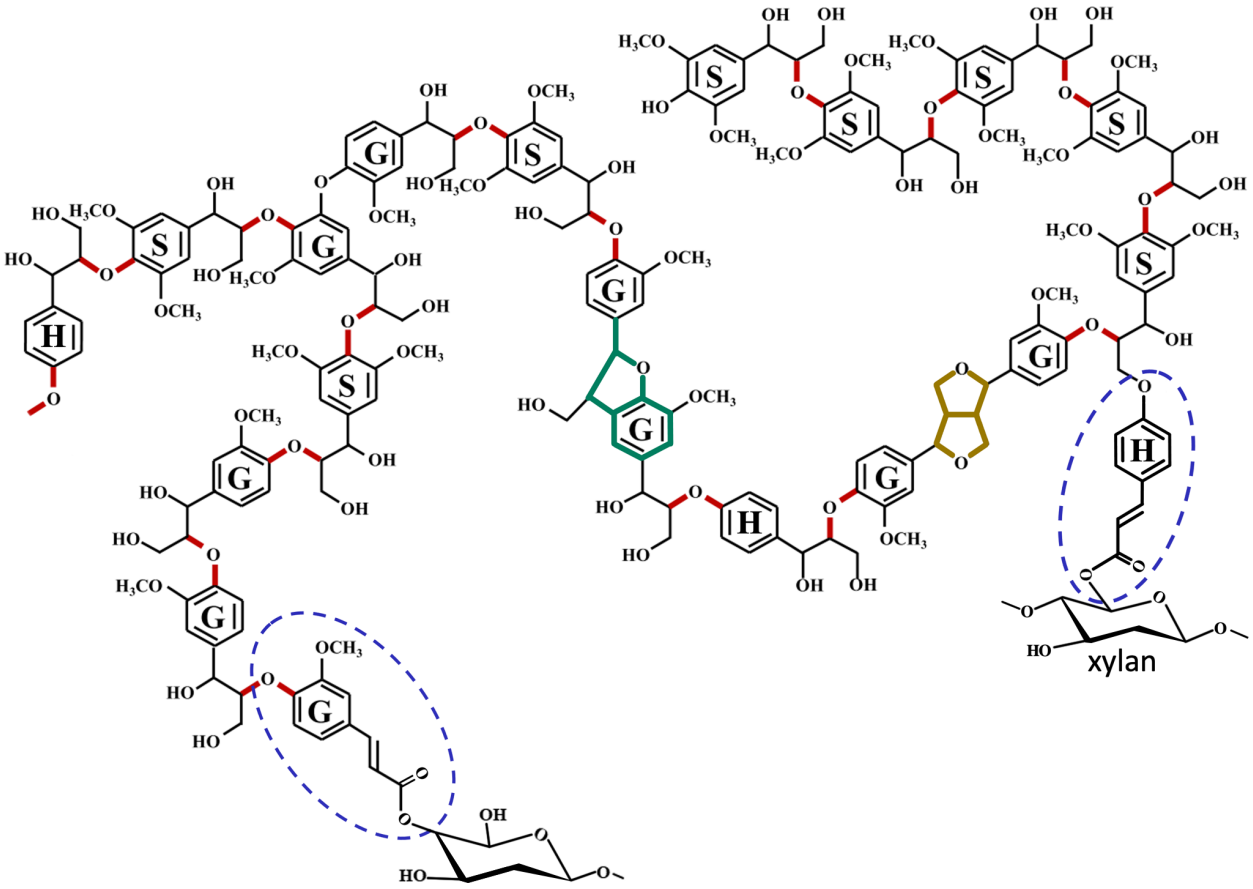

Figure 1.5: Generic structure of a grass lignin (Jasiukaitytė-Grojzdek et al., 2020). (red: β-O-4′; yellow: β-β' resinol; green: β-5′ phenylcoumaran; blue: ferulate esterase LCC)

occur less frequently (Ma et al., 2018; Vanholme et al., 2008). The most prolific motif, β-O-4′ (β-aryl ether), accounts for 40-60% of all linkages. α-O-4′ (α-aryl ether) and β-5′ + α-O-4′ (phenylcoumaran) are similar ether motifs. Other prevalent motifs include β-β' (resinol), β-5′ (diphenyl propane), 4-O-5′ (diaryl ether), α-O-γ' (aliphatic ether), and 5-5′ (biphenyl) but exist minimally across all species (Vanholme et al., 2019; Azadi et al., 2013; Wei Kit Chin et al., 2020; Tocco et al., 2021). Grass lignins contain a unique motif, tricin, which exclusively bonds via a reverse β-O-4′ linkage from its own phenyl to another β-carbon in lignin (Tocco et al., 2021).

Alkyl-aryl ether bonds are particularly acid-labile, thus β-O-4′ bonds are frequently broken during most pretreatments. The bond-dissociation energy (BDE) of β-O-4′ (215 KJ/mol) and α-O-4′ (290 KJ/mol) are roughly half of their alkyl counterparts (e.g., 530 KJ/mol for β-5′) (Guadix-Montero and Sankar, 2018; Vanholme et al., 2008). Cleavage of β-O-4′ bonds leads to condensation reactions under organosolv conditions (Jasiukaitytė-Grojzdek et al., 2020).

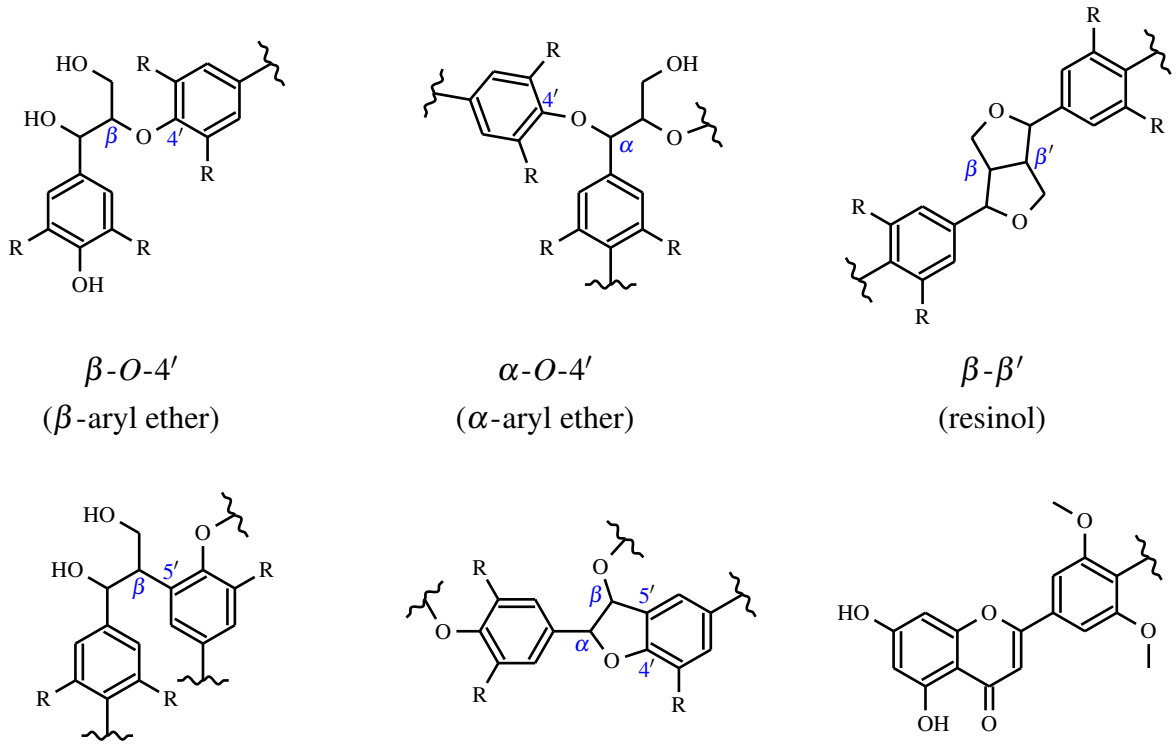

Figure 1.6: Common structural motifs found in grass-type lignins

Table 1.4: Composition of structural motifs in various biomass sources (Wei Kit Chin et al., 2020; Azadi et al., 2013; Rinaldi et al., 2016).

Linkage	**Name**	**Softwoods (%)**	**Hardwoods (%)**	**Grasses (%)**
β-O-4′	β-aryl ether	45-50	60-62	74-84
α-O-4′	α-aryl ether	2-8	7	3-9
β-β′	resinol	2-6	3-12	1-7
β-5′	diphenyl propane	7	7	1-8
β-5′ + α-O-4′	phenylcoumaran	9-12	3-11	5-11
4-O-5′	diaryl ether	2-4	2-7	n.d.
5-5′	biphenyl	5-11	1-5	n.d.
-	tricin	n.d.	n.d.	1-16

1.3.1.3 Lignin–Carbohydrate Complexes

Inside the lignocellulose matrix, hemicellulose and lignin bond in unique motifs called *lignin-carbohydrate complexes* (LCCs) (Karlen et al., 2016). These complexes (Figure 1.7) can include benzyl ether, benzyl ester, glycosidic or phenyl glycosidic, hemiacetal or acetal, ferulate or coumarate esters motifs (Tarasov et al., 2018; Buranov and Mazza, 2008). While these are mostly traditional lignin motifs, the ferulate and coumarate esters are atypical.

Herbaceous LCCs differ from wood LCCs in both form and abundance (Tarasov et al., 2018; Karlen et al., 2016). Woody species contain ether, ester, and glycosidic LCCs, though scarcely. Conversely, LCCs are more abundant in non-woody plants but predominantly appear as ferulates or coumarates esterified to xylans (Buranov and Mazza, 2008). Such motifs are known as *lignin-ferulate-carbohydrate complexes* (LFCCs), appearing in Figures 1.2 and 1.5. As highly alkali-liable, retention of LFCCs is varied across technical lignins (Tarasov et al., 2018). LFCCs can be found in organosolv lignins of herbaceous species. Corn residues, for example, contain up to 4-8% and 1-3% of the coumarate and ferulate varieties, respectively (Min et al., 2014). The alkene of LFCCs enables a valorization chemistry that is not possible with wood lignins.

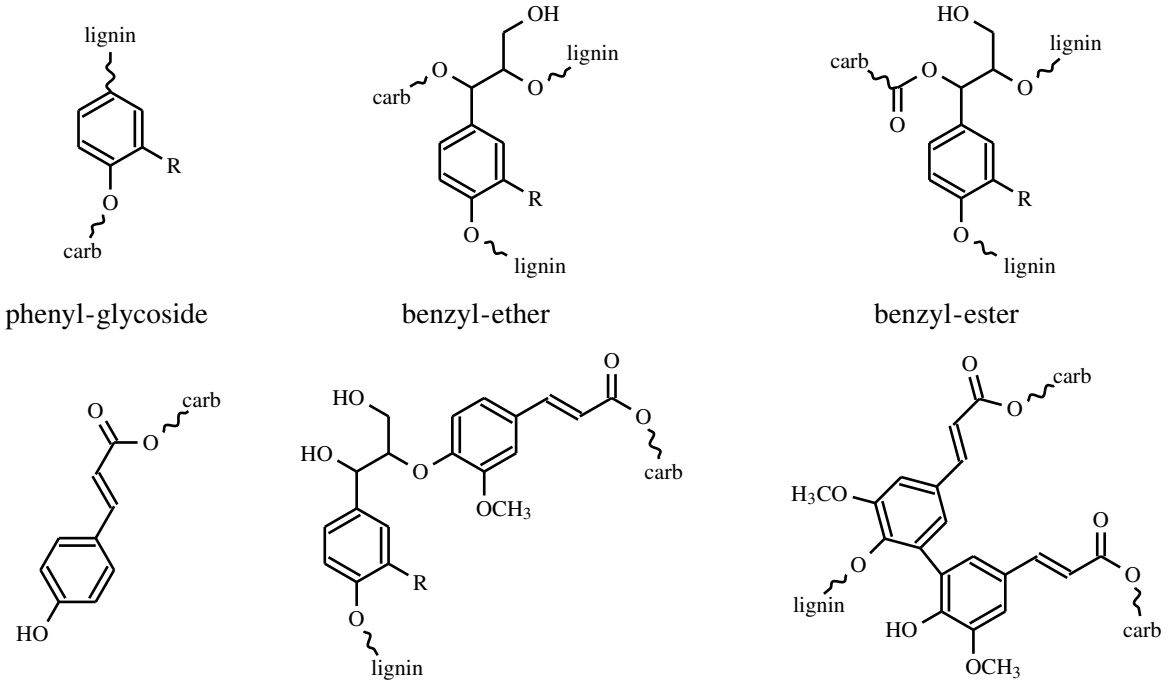

Figure 1.7: Several known lignin-carbohydrate complexes (Tarasov et al., 2018).

Like lignin biosynthesis, biosynthesis of LCCs is out of scope for this work, and the reader is encouraged to refer to Karlen et al. (2016), Vanholme et al. (2019), and Tarasov et al. (2018).

1.3.2 Lignin Applications

Despite the extensive markets for cellulose and hemicellulose, lignin has for decades been considered a nuisance byproduct. Heterogeneity and multifunctionality, properties inherent to lignin, have thus far hindered attempts to valorize lignin. Instead, nearly all lignin ends up as low-grade fuel with a heat value of 25 MJ/kg (Bajwa et al., 2019). Excluding fuel, the majority of lignin's market (85%) is occupied by the only presently-viable technical lignin, lignosulfonate (Grand View Research, 2020). Other lignins have yet to be commercialized.

Starting from $950 million in 2019, the global market of lignin is expected to rise at a compound annual growth rate (CAGR) of 2.0% from 2020-27. Applications of lignin may be categorized as monomer extractions or polymeric substitutions. In 2020, polymeric applications were 58% of the market which slightly edge out monomers at 42% (Grand View Research, 2020).

Some lignins can substitute petrochemicals as an inexpensive filler or additive for resins and adhesives, similar to its natural function. By manipulating lignin's reactive side-chains, its adhesive properties can be made suitable for resins in plywood, particle board, synthetic fibers, plastics, and electrical insulation (Wild et al., 2014; Silverman et al., 2020). In some intriguing applications, lignin may induce desirable properties such as water resistance, biodegradability, and fire retardation (Gandini and Belgacem, 2008; Mandlekar et al., 2018).

Lignin's greatest value lies in its abundant aromatic monomers. A number of lignin technologies afford commodity chemicals such as benzene, toluene, and xylene (BTX) and phenol (Wild

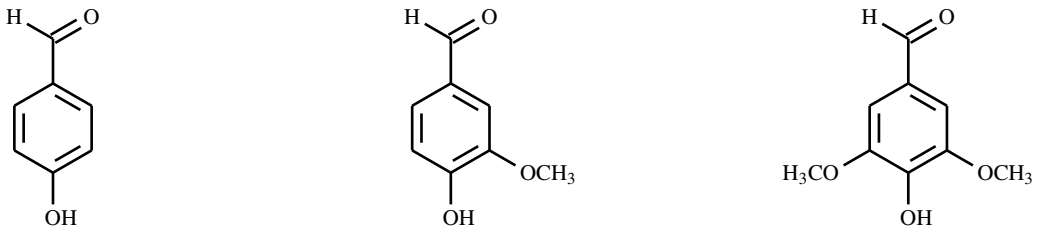

(a) *p*-hydroxybenzaldehdye (b) vanillin (c) syringaldehyde

Figure 1.8: Flavoring agents which may be extracted from lignin.

et al., 2014; Sun et al., 2018). Lignin may one day be a renewable feedstock for such platform petrochemicals. In the past, specialty chemicals including *p*-hydroxybenzaldehyde, vanillin, and syringaldehyde (Figure 1.8) were commercial products of lignin (Den et al., 2018). Other niche applications include membranes, energy storage composites, and carbon fiber (Rinaldi et al., 2016).

1.3.2.1 Vanillin

Since the 1920s, vanillin has been commercially produced from lignin to some extent (Zabkova et al., 2007). As the major constituent of vanilla, vanillin's applications extend from flavorings to fragrances to pharmaceuticals (Walton et al., 2003). Natural vanilla derived from vanilla orchids accounts for <1% of vanillin production. The remaining demand is met via synthetic vanillin from petrochemicals, e.g. guaiacol, and lignin to a lesser degree (Walton et al., 2003; Zabkova et al., 2007). Figure 1.9 illustrates several synthetic pathways for vanillin from several petrochemicals.

In theory, lignin could be a sustainable alternative for vanillin production. However, the now-obsolete technologies required excessive volumes of caustic soda for meager yields. Hence, much of the vanillin-from-lignin industry ceased production in the 1990s. Børregaard (Norway) is one of the few remaining producers of vanillin from lignin (Hocking, 1997; Rinaldi et al., 2016). Today, lignin-derived vanillin accounts for ca. 15% of the market (Van den Bosch et al., 2018).

Vanillin's global market size was just under $600 million in 2019 and is projected to reach $1.72 billion in 2027 with a CAGR of 14.1% (Reports and Data, 2020). An estimated 50% of the

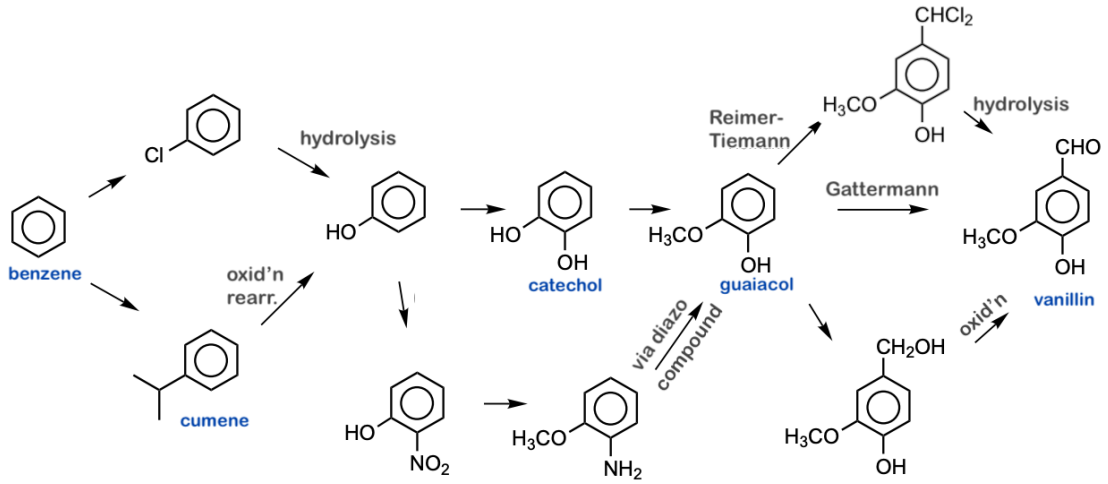

Figure 1.9: Pathways to synthesize vanillin from petrochemical feedstocks (Hocking, 1997).

production, and growing since 2003, was anticipated for pharmaceuticals, antimicrobials, and other speciality chemicals (Walton et al., 2003). Vanillin was recently explored as a polymer additive as well (Imre and Pukánszky, 2015; Amarasekara et al., 2012). Novel technologies for sustainable vanillin production from lignin could carve out much of the petrochemical's market share.

1.3.2.2 Phenolic Resins

Lignin's largely phenolic structure makes it a clear substitute in phenol-formaldehyde (PF) or similar phenolic resins (Bajwa et al., 2019; Gandini and Belgacem, 2008). Rather than complementing the PF chains, lignin supplants up to 80% of the phenol in these lignin-phenol resins (Figure 1.10). Modifying the lignin before substitution may afford tailored polymers like novolac-type or resol-type PF resins (Wild et al., 2014). Silverman et al. (2020) extracted and then grafted endogenous phenolic aldehydes back onto the lignin's backbone to afford novolac-type PF resins. Other treatments such as methylolation or oligomeric co-reagents have been explored (Gandini and Belgacem, 2008). The resurgence of PF resins in products like circuit board insulation, particle boards, fibre boards, and varnishes over the past decade may be attributed to these new technolo-

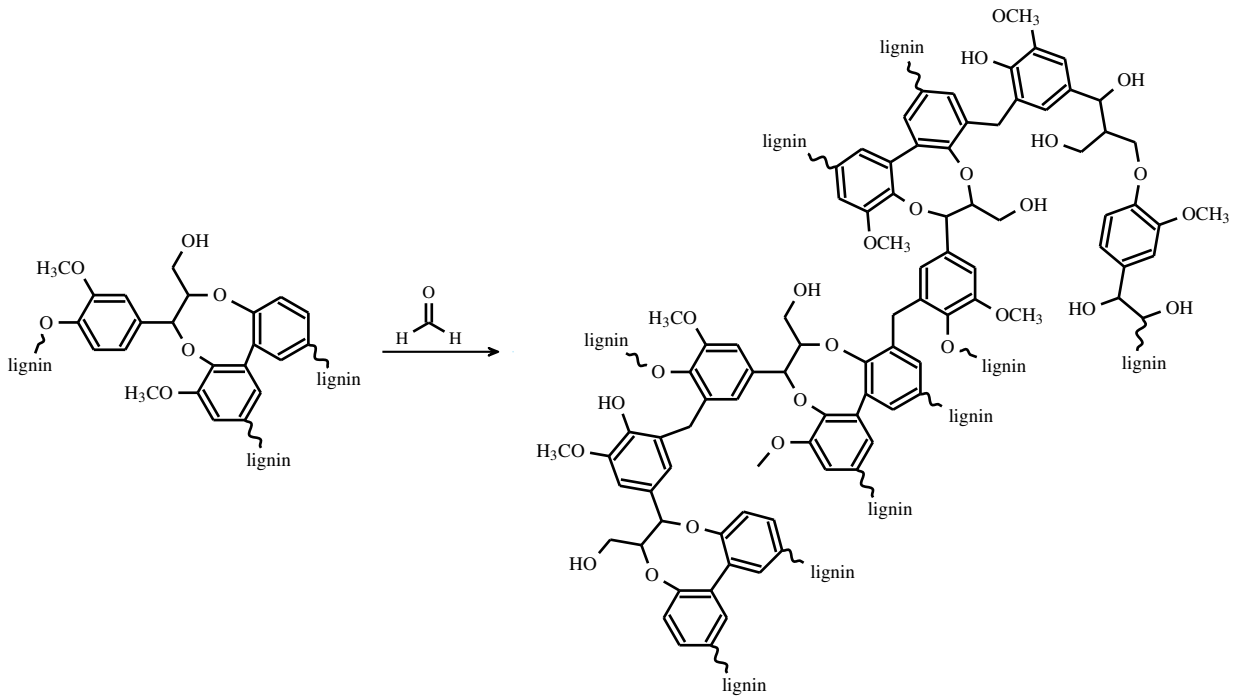

Figure 1.10: General scheme for the addition of formaldehyde to phenolic lignin to form lignin-based phenol-formaldehyde resins (Upton and Kasko, 2016).

gies (Wild et al., 2014). Grand View Research (2020) projected the global market of phenolic resins to rise at 6% CAGR through 2024 from its estimate of $4.56 billion in 2020.

1.4 Lignin Valorization

Conventionally, valorization technologies focus on the technical lignins as an isolated byproduct independent of the other fractions. Thus, complete valorization of biomass is a combination of fractionation and subsequent individual valorization technologies. However, a new field guided by a *lignin-first* dogma is emerging (Abu-Omar et al., 2021). These approaches transform lignin in place without the need to isolate it from cellulose and hemicellulose. Comparatively high yields of monomers have been demonstrated, but the cellulose and hemicellulose are severely degraded as well. Hence, *lignin-first* approaches should be considered a corollary to traditional fractionation-then-valorization rather than a replacement.

More traditional valorization strategies depolymerize lignin to differing extents under various process conditions. Nearly all methods utilize oxidation or reduction under low-severity (mild) or high-severity (harsh) conditions. Products of mild conditions include aromatic monomers whereas non-aromatic monomers such as small carboxylic acids are produced under harsh conditions (Rinaldi et al., 2016). Some enzymatic processes have also been demonstrated. In a thorough review, Schutyser et al. (2018) determined the median yield of any pathway rarely exceeded 20 wt.%.

1.4.1 Oxidative Pathway

Oxidation is generally the most common and successful lignin depolymerization strategy (Den et al., 2018). Low-severity oxidative cleavage affords methoxyphenol monomers with added functionality such as aldehydes, ketones, and carboxyls (Ma et al., 2018; Van den Bosch et al., 2018). High-severity conditions will further oxidize such phenolics into aliphatic carboxylic acids. Although not mandatory, catalysts significantly aid in overcoming lignin's natural chemical resistance (Schutyser et al., 2018). Monomer yields have been improved using catalysts such as organometallic, metal-free organic, and acid or base catalysts (Sun et al., 2018; Van den Bosch et al., 2018).

Aromatic monomers result from the extensive breakage of aryl-ether bonds (β-O-4′ and α-O-4′) prevalent in low-severity oxidation. Sadly, β-O-4′ cleavage routinely results in undesired condensation reactions. Conditions for low-severity typically range from 175-250 ºC and O_2 pressures of 2-15 bar (Van den Bosch et al., 2018). Oxidation processes typically target phenolic aldehyde or acid as high-value products (Banu et al., 2019). Thus, primary products are *p*-hydroxybenzaldehyde (*p*HB), vanillin, and syringaldehyde. The monomer ratios are predicted by the H/G/S content of the lignin feedstock (see Table 1.3). For oxidation, aromatic monomer yields rarely exceed 20 wt.% and typically are below 15 wt.% (Van den Bosch et al., 2018).

As reaction severity increases, the stability of phenolic monomers decreases as their aromatic rings become increasingly susceptible to degradation (Schutyser et al., 2018). Hence, the H/G/S content has little impact on the products whereas reaction media and process conditions are the foremost influence. Products of high-severity approaches include small-chain carboxylic acids such as formic, acetic, oxalic, malonic, and succinic acids (Banu et al., 2019). High-severity is typically reached with high O_2 pressure, long reaction time, or low pH. As opposed to O_2, peroxides (e.g. H_2O_2) are more common in high-severity conditions (Van den Bosch et al., 2018).

Several detailed reviews on lignin oxidation are available, Li et al. (2015); Ma et al. (2018); Rinaldi et al. (2016); Banu et al. (2019); Cheng et al. (2017)

1.4.1.1 Alkaline oxidation

Historically, commercial-scale alkaline oxidation produced vanillin from lignin using caustic soda and oxygen under low-severity conditions (Schutyser et al., 2018). Depending on the lignin feedstock, *p*HB and syringaldehyde could also be produced. These processes often have poor selectivity leading to noticeable conversion of the aldehydes to their carboxylic acid derivatives. Monomer yields have been reported up to 10-20 wt.%, but yields below 10 wt.% are more typical (Van den Bosch et al., 2018).

Homogeneous and heterogeneous transition metal catalysts are known to enhance reactivity of oxygen in alkaline oxidation. Typical metals include Fe^{III}, Mn^{II}, Mn^{III}, Co^{II}, and Zr^{IV} (Liu et al.,

2020). Heterogeneous metal oxides including CuO, MnO_2, TiO_2 and ZnO have been employed in some commercial processes (Liu et al., 2020; Van den Bosch et al., 2018; Tarabanko et al., 2004). Complex materials such as Cu-doped perovskites, polyoxometalates, biomimetic catalysts have seen success but lack commercial usage (Liu et al., 2020; Banu et al., 2019). Due to Børregaard's success, Cu^{II}-catalyzed oxidation in NaOH is the most common process (Liu et al., 2020).

Oxygen is typically insufficient to ionize lignin's phenolic hydroxyls into phenolate ions, hence high-pH media is used to facilitate ionization and initiate depolymerization (Schutyser et al., 2018). The alkaline media may also inhibit further degradation of the monomer products at low-severity. High temperature or O_2 pressure accelerates phenolic aldehyde formation, but this inevitably accelerates their degradation into carboxylic acids (Van den Bosch et al., 2018). Complex carboxylic acids such as oxalic and glutaconic acids are favored in high-severity but low temperatures (ca. 200 ºC). At higher temperatures, formic, acetic, and succinic acids are favored products (Van den Bosch et al., 2018). Monomer yields of up to 56 wt.% have been reported (Schutyser et al., 2018).

1.4.1.2 Acidic oxidation

For some technical lignins, acidic media can improve critical process conditions including solubility. Dilute inorganic acids and concentrated small carboxylic acids are popular in acidic oxidation schemes (Van den Bosch et al., 2018). The acidity may influence product selectivity and catalyst selection, but the process and products are typically identical to alkaline oxidation. Phenolic acids tend to be the dominant product of acidic oxidation due to the over oxidation of the phenolic aldehydes (Schutyser et al., 2018). With optimal design, phenolic aldehydes may be selectively produced instead. In such processes, Kraft lignin and softwood lignosulfonates can yield vanillin and methyl vanillate. Typical monomer yields are around 9-15 wt.% in acidic media but can reach up 20 wt.% monomers (Schutyser et al., 2018).

Studies show that metal salt catalysts ($CuSO_4$ and $CoCl_2$) can improve production rates in H_2SO_4 media (Cheng et al., 2017). In contrast, $CuCl_2$ and $FeCl_3$ did not increase yields but shortened reaction time instead (Li et al., 2015). Catalysts containing Co/Mn/Zr/Br salts are also preva-

lent. Studies of Zr-based solid acid catalysts (e.g., Zr-KIT-5) demonstrated yields up to 28 wt.% monomers (Nandiwale et al., 2017, 2019). Other works suggest that co-solvents (e.g., methanol) enhance yields due to potential mechanistic influences (Li et al., 2015; Schutyser et al., 2018).

1.4.1.3 Oxidation in Ionic Liquids

Ionic liquids (ILs) have driven the recent growth in popularity of pH-neutral oxidation (Dai et al., 2016). Other media have poor control over condensation reactions and the extent of oxidation to the products. However, ILs can be designed to be effective lignin solvents that overcome these shortcomings while affording similar products. For grass and softwood lignins, oxidation in ILs yields unsubstituted methoxyphenols and phenolic aldehydes (Schutyser et al., 2018).

To date, studies of ILs with technical lignins are limited. This lack of breadth contributes to inconsistencies and large variability in the performance of ILs (Chatel and Rogers, 2014). Generally, vanillin yields are enhanced when ILs are used in combination with $CuSO_4$. In a mixture of $[C_1C_1im][Me_2PO_4]$/MIBK, $CuSO_4$-catalyzed oxidation of organosolv lignin at 175 ºC achieved up to 30 wt.% monomers (Schutyser et al., 2018). In another study, organosolv lignin yielded only 12 wt.% monomers when oxidized in $[C_2C_1im][CF_3SO_4]$ with $Mn(NO_3)_2$ at 100 ºC. In contrast, oxidation in $[HC_4im][HSO_4]$ at 100 ºC afforded <1 wt.% of monomers (Chatel and Rogers, 2014).

Dai et al. (2016) and Chatel and Rogers (2014) review lignin and ILs in much greater detail.

1.4.1.4 Non-Catalytic Oxidation with Ozone

Practical non-catalytic strategies rely on the use of more powerful oxidizing agents. While presently uncommon, ozone is one such highly reactive oxidizing agent. Ozone enables a unique depolymerization chemistry that shifts the cleavage away from the β-O-4′. As described by the Criegee mechanism, ozone preferentially attacks C=C (Criegee, 1975). Being mostly aromatic, lignin is susceptible to ring-opening reactions and severe depolymerization given sufficient contact time and conditions. With proper design, the reaction can be engineered to minimize ring-opening and instead target alkene bonds that may be present in lignin (Danby et al., 2018). While alkene

bonds are not present in woody lignins, grass lignins contain appreciable quantities that can yield phenolic aldehydes. The process can be intensified at ambient conditions to produce up to 6 wt.% of monomers from grass lignins (Danby et al., 2018; Silverman et al., 2019).

1.4.2 Reductive Pathway

Another viable depolymerization is the reductive cleavage of lignin's aryl-ether linkages. Because the reducing agent is nearly exclusively hydrogen gas, most reductive strategies are synonymous with hydroprocessing (Van den Bosch et al., 2018). Similar to oxidation, low-severity and high-severity reduction afford aromatic monomers and small carboxylic acids, respectively. However, catalysts are essential for reductive pathways. Traditional hydroprocessing uses noble metal or base metal catalysts (Schutyser et al., 2018). Bifunctional catalysts are growing in popularity due to their distinctive monomer products. Some examples are noble metals supported on zeolites including Pt/HY, Ru/HZSM-5, and Pd/HY (Banu et al., 2019; Van den Bosch et al., 2018).

Depolymerization proceeds via the cleavage of prominent β-O-4′ and α-O-4′ motifs and removal of side-chain hydroxyls (Schutyser et al., 2018). To a lesser extent, aromatic rings and $C{=}O$ or $C{=}C$ bonds are also hydrogenated (Van den Bosch et al., 2018). Yet, much of the aliphatic side-chain remains intact because the $C{-}C$ bonds resist reduction (Schutyser et al., 2018). The extent of side-chain functionalization is inversely related to the monomer value from reduction as opposed to directly related in oxidation (Liu et al., 2020).

Other reductive pathways exist but are infrequently used, such as hydrodeoxygenation (HDO) (Liu et al., 2020). Liquid-phase reforming, a subset of hydroprocessing, utilizes internal hydrogen-donors such as lignin itself or the solvent (Schutyser et al., 2018). Rinaldi et al. (2016), Banu et al. (2019), and Li et al. (2015) extensively review reductive depolymerization of lignin.

1.4.2.1 Mild Hydroprocessing

Mild hydroprocessing constitutes conditions below 300 ºC, resulting in the preservation of methoxyl groups on the aryl rings (Banu et al., 2019; Schutyser et al., 2018). Para-substituted

methoxyphenols are the primary products, but the catalyst has a demonstrated effect on the monomer type and yield (Schutyser et al., 2018). For example, Cu/PMO-catalyzed mild hydroprocessing of candlenut lignin in methanol is reported to yield up to 64 wt.% of substituted catechols (Liu et al., 2020). Lewis acid co-catalysts are also suggested to enhance productivity. Yields from softwood alkali lignin increased from 7 to 29 wt.% when $CrCl_3$ was added to Pd/C (Schutyser et al., 2018).

A fundamental relationship may be drawn between (1) high β-O-$4'$ content and (2) high monomer yields. In the same vein, hydroprocessing of lesser condensed lignins may lead to higher retention of side-chain functionality on the methoxyphenols (Schutyser et al., 2018).

1.4.2.2 Harsh Hydroprocessing

Harsh hydroprocessing at higher than 320 ºC and 35 bar of hydrogen results in the methoxy groups not being preserved (Banu et al., 2019). Hence, phenol and alkyl substituted phenols are the primary products of low-end harsh conditions (Schutyser et al., 2018). Poor selectivity accompanies high-severity thus an array of monomers are formed such as (poly)cyclic deoxygenated aromatics, alkanes, and catechols (Schutyser et al., 2018). Amongst the possible noble metal and base metal catalysts, CoMo and NiMo are frequestly reported (Schutyser et al., 2018).

Uniquely, harsh hydroprocessing does not require solvents (Van den Bosch et al., 2018). Several studies report substantial yields when using solid catalysts without solvents. For example, solvent-free conversion of hardwood organosolv lignin produced 22 wt.% monomers at 400 ºC catalyzed by Ru/C, Ru/TiO_2, or Pd/C. Similarly, pine Kraft lignin yielded 26 wt.% monomers at 350 ºC with sulfided Ni/Mo/MgO-La_2O_3 (Schutyser et al., 2018).

1.4.2.3 Liquid-Phase Reforming

Liquid-Phase Reforming (LPR) is a variant of hydroprocessing where the hydrogen-donor is the solvent, dissolved in the solvent, or, in some cases, from lignin itself (Schutyser et al., 2018). Solvent-derived hydrogen permits lower temperatures, thus improving inherent safety (Van den Bosch et al., 2018). Monomer products of LPR include alkyl-substituted methoxyphenols, cate-

chols, alkylphenols, deoxygenated aromatics, and cycloalkanes (Banu et al., 2019). With the same substrate, LPR often achieves larger yields (ca. 20 wt.%) than hydroprocessing (Schutyser et al., 2018). For instance, hyroprocessing Kraft lignin yielded only 4-6 wt.% compared to 18 wt.% recovered by LPR with H_2SO_4 and the same Pt/Al_2O_3 catalyst (Rinaldi et al., 2016).

Noble and base metal catalysts (e.g., Pt, Pd, Ru, $CuMgAlO_x$) appear to be best suited for LPR (Van den Bosch et al., 2018). Small carboxylic acids and alcohols are typical solvents, hence most studies report using methanol, ethanol, isopropanol, formic acid, tetralin, or ethylene glycol (Schutyser et al., 2018). Regeneration of the oxidized solvent, often requiring an external reducing agent (e.g., H_2), is a clear disadvantage of LPR (Van den Bosch et al., 2018).

As a reaction participant, solvent selection directly impacts monomer yields. Methanol produced only 6 wt.% compared to 17 wt.% using ethanol in $CuMgAlO_x$-catalyzed LPR of wheat straw lignin (Schutyser et al., 2018). The results suggest ethanol impeded condensation reactions by scavenging formaldehyde and alkylating phenolics at condensation-prone positions (C_3-C_5) (Van den Bosch et al., 2018). Similarly, MoC/C-catalyzed LPR of softwood lignin performed best in ethanol (28 wt.%) compared to methanol, isopropanol, and water (Schutyser et al., 2018).

1.4.2.4 Reductive Catalytic Fractionation

To this point, valorization strategies have targeted the technical lignins. Reductive Catalytic Fractionation (RCF) diverges from this dogma by targeting the unfractionated lignin ('protolignin') (Van den Bosch et al., 2018). RCF combines simultaneous solvolysis and heterogeneous redox-catalyzed hydroprocessing to yield significant quantities of monomers, dimers, and oligomers (Schutyser et al., 2018). In addition to the selective production of *p*-substituted methoxyphenols, the remaining pulp contains additional value in carbohydrates (Liu et al., 2020). The reducing agent of RCF is almost exclusively hydrogen. Similar to LPR, the hydrogen can be sourced externally or supplied by a hydrogen-donating solvent or the lignin itself (Schutyser et al., 2018). Common variations use methanol, isopropanol, or other small alcohols, but aqueous organic solvents are also reported (Liu et al., 2020; Schutyser et al., 2018).

RCF originates from a discovery in a study of conventional hydroprocessing and beech wood. When using sulfided NiMo/γ-Al_2O_3, organosolv beech lignin only produced 4.3 wt.% while untreated beech wood chips could reach 18.1 wt.% monomers. This result highlighted the challenges of technical lignins; extracting lignin unavoidably induces condensation reactions and recalcitrance (Liu et al., 2020). RCF circumvents the issue by in-situ cleavage of β-O-4′ linkages in their native state (Sun et al., 2018). Catalytic reduction inherently stabilizes alkenyl and carbonyl intermediates which would otherwise lead to condensation reactions (Schutyser et al., 2018; Liu et al., 2020).

Standard RCF catalysts are metals including Ru, Pd, Rh, and Ni on activated C or Al_2O_3 supports (Sun et al., 2018). Catalyst selection influences several factors including monomer selectivity and yield, fractionation efficiency, and process severity. Inexpensive Ni/C catalyst afforded 89% selectivity toward propyl-substituted guaiacol and syringol (Song et al., 2013). Similar selectivity could be achieved with Ru/C, Pt/C, or Rh/C which also removed the γ-hydroxyls and Pd/C or Raney Ni catalysts which formed propanol-substituted monomers (Van den Bosch et al., 2018).

Unique to RCF, a theoretical yield of monomers can be predicted by the contents of S-units in the feedstock's lignin (Sun et al., 2018; Van den Bosch et al., 2018). Indeed, studies show that RCF of hardwoods yields 40-55 wt.% monomers while softwoods yield <30 wt.% (Van den Bosch et al., 2018). These yields align with the S-unit values reported in Table 1.3. Herbaceous feedstocks are less consistent, as the yields typically range from 20-40 wt.% (Schutyser et al., 2018).

1.4.3 Enzymatic Pathway

Enzymes have demonstrated various capacities to valorize biomass. Hydrolytic enzymes can readily depolymerize starch and cellulose, but their efficacy is hindered by lignin's heterogeneity and complexity (Kumar et al., 2009; Houfani et al., 2020). Some species of fungi and bacteria produce enzymes that are capable lignin degraders, peroxidases and laccases (Houfani et al., 2020). Most bacteria are reported to produce both versatile peroxidase and dye-decolorizing peroxidase (Banu et al., 2019). Fungi tend to be more effective producers, but bacteria achieve higher conversion rates. Unlike bacteria, fungi produce both laccases in addition to stronger peroxidases,

lignin peroxidase and manganese-dependent peroxidase (Banu et al., 2019). As such, white rot and brown rot fungi are highly active lignin degraders (Janusz et al., 2017; Wen et al., 2009).

Enzymes convert lignin to oxygenated products such as phenolic aldehydes and acids or, with some bacteria, polyhydroxyalkanoates (PHAs). When fermented with *Aspergillus fumigatus*, lignin-rich wheat straw produced vanillic acid and other small carboxylic acids (Banu et al., 2019). One bacterium, *Pseudomonas putida KT2440*, yielded 34-39 wt.% of medium-chain PHAs (Sun et al., 2018). Some strains may yield smaller quantities of PHAs but convert more lignin which could be used in a two-stage valorization process. For instance, *Amycolatopsis sp.* can reach 30 wt.% conversion (Rinaldi et al., 2016).

Additional information can be found in the reviews on enzymatic valorization of lignin by Janusz et al. (2017) and Banu et al. (2019)

1.5 Objective

The sustainable success of biorefineries depends upon the valorization of all lignocellulose fractions of biomass. Despite their prevalence, Kraft and sulfite pulping fail to maintain the value of all lignocellulosic fractions (namely, lignin) due to destructive processing. To develop technologies for the complete utilization of biomass, cleaner and less destructive preteatments must be employed. One such pretreatment, the acetosolv process, efficiently fractionates lignocellulose with minimal degradation. Practical applications of traditional lignin fractions are limited, but the aromaticity retained in the acetosolv lignin affords substantial value if utilized correctly.

Valorization of lignin has been demonstrated with a variety of approaches from oxidative to reductive to biological but often fail to produce a value greater than the operational cost. Technologies that do produce value are unselective and yield complex product mixtures thus requiring costly separations. New lignin-first methods such as RCF are only suitable for low-grade lignocellulose where the fiber grade is inherently low. Alternatively, fast ozonolysis has demonstrated the ability to selectively extract high-value monomers from lignins derived from high-grade lignocellulose in corn stover (Danby et al., 2018). Spray ozonolysis of acetosolv lignin affords vanillin

and *p*HB while preserving the macrostructure of the lignin (Silverman et al., 2019). However, an understanding of this process aimed at practical aspects is still lacking.

In this work, we investigate the viability of ozonolysis on an alternative corn residue, corn cobs. The versatility of spray ozonolysis is evaluated with lignins from corn cobs and corn stover that were extracted using a large lab-scale acetosolv process developed in this work. Application of ozonolysis on emerging feedstocks other than corn residues strengthens its case for commercialization. As such, we investigate the structure of acetosolv lignin to reveal insights which may correlate with the performance of any potential feedstock. Determining such a correlation will greatly limit costly research expenditure. Further, studies were carried out to determine the effect of the spray reactor's operating parameters on the product yield. The results of these studies will inform a rational approach to process development aimed at eventual commercialization.

Chapter 2

Acetosolv Extraction of Lignin from Corn Cobs

2.1 Background

Field residues of corn are an exceptionally underutilized source of lignocellulose that may find use in biorefineries. Harvesting corn grain produces an equal mass of non-grain residues (stalks, leaves, husks, and cobs) (Shinners and Binversie, 2007; Blandino et al., 2016). In the U.S., this equates to more than 380 million tons of unused lignocellulose annually. (NASS, 2021, 2019). The typical composition of corn residues and combined lignocellulose are expressed in Figure 2.1. Domestic cellulose industries could annually generate up to 70 million tons of lignin from corn residues (Blandino et al., 2016; Pordesimo et al., 2002; Birrell et al., 2014). Due to adaptable agronomy and annual growth, corn is globally recognized as an ideal natural resource. Achieving an economically viable valorization of such a resource in a sustainable manner (i.e., minimizing adverse ecological and anthropological impacts) not only rejuvenates a struggling industry but also establishes innovative domestic manufacturing capacity in the chemical sector.

Optimal valorization of corn residues necessitates a pretreatment with minimal degradation to *all* lignocellulose fractions. To reach lignin's greatest value potential, the pretreatment must yield

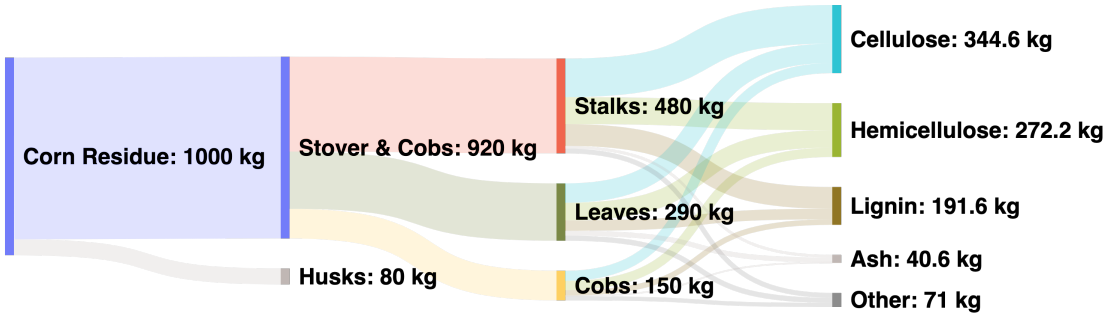

Figure 2.1: Distribution of composition in corn residues.

a technical lignin with limited condensation and free of sulfur. The organosolv process is one such pretreatment that meets these criteria. Ethanol biorefineries may find these characteristics to be particularly attractive (Danby et al., 2018).

Owing to its capacity to solubilize lignin and low cost, organosolv processes often prefer aqueous acetic acid which is known as the acetosolv process (Ragauskas et al., 2014; Liao et al., 2020; Budzinski and Nitzsche, 2016). Historically, the commercial application of acetosolv process has been limited due to energy costs and insufficient valorization of non-cellulose streams (Kautto et al., 2014). Yet, acetosolv fractions are food-safe and potentially contain more value than traditional pretreatments. If practically viable valorization techniques are developed, biorefineries may adopt the acetosolv process as a greener alternative to traditional sulfur-based treatments.

2.1.1 Physicochemical Mechanism

The primary mechanism of acetosolv fractionation is the solvolytic hydrolysis of inter-unit linkages between cellulose, hemicellulose, and lignin. Aqueous acetic acid catalyzed by sulfuric acid simultaneously breaks these bonds and solubilizes the liberated lignin and hemicellulose. Figure 2.2 illustrates the general scheme of the hydrolysis reaction.

Fractionation primarily proceeds via the breakage of β-aryl ether bonds to form benzylic car-

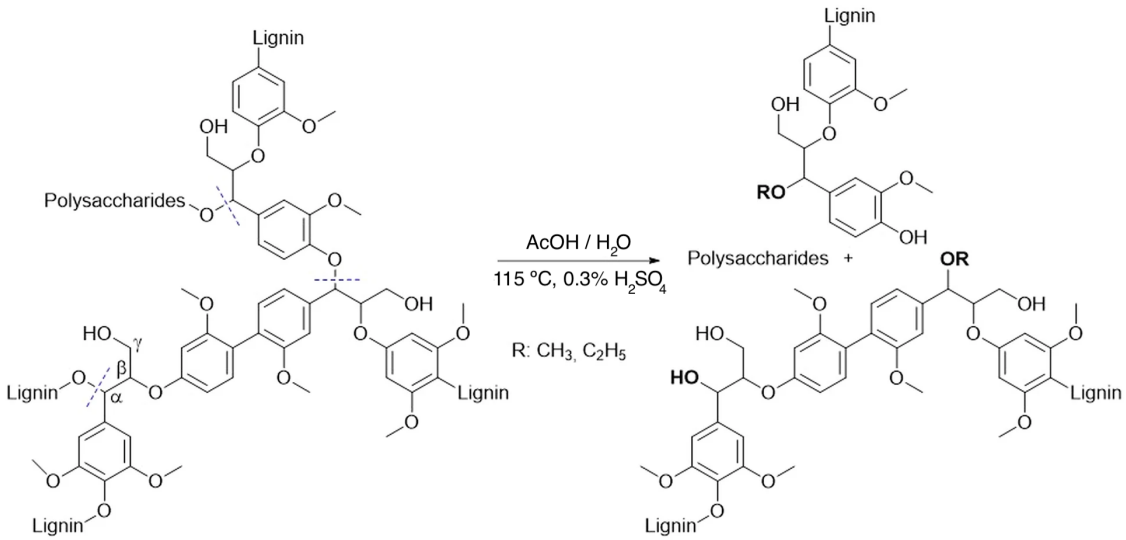

Figure 2.2: Reaction scheme for the solvolytic hydrolysis of lignin during the acetosolv process (Jasiukaitytė-Grojzdek et al., 2020).

bocations (Kangas et al., 2015). Due to differences in bond dissociation energy (BDE), α-O-4′ bonds (215 kJ/mol) are cleaved prior to β-O-4′ scission (290 kJ/mol) during initial hydrolysis (Jasiukaitytė-Grojzdek et al., 2020). The carbocations are susceptible to nucleophilic addition reactions to eventually form condensed β-aryl bonds (Kangas et al., 2015). Hibbert ketones may also form via aryl-enol intermediates and γ-carbon cleavage, but these are prone to condensation reactions. By using aqueous acetic acid, alkoxylation of the side-chains can be avoided thus preserving the lignin's hydroxyl functionality (Jasiukaitytė-Grojzdek et al., 2020).

2.2 Experimental

2.2.1 Sourcing Corn Residues

Corn cobs used for extractions in this work were supplied by J-Six Enterprises, a corn cob processor, located in Seneca, Kansas. Commercial samples of acetosolv lignins from corn cobs and corn stover were provided by Archer Daniels Midland Company (ADM). The acetosolv extraction used by ADM is similar to the process described in this study. Details of this work were provided by the industry mentors of this work (Binder and Hagberg, 2020).

2.2.2 Developing a Large Lab-Scale Acetosolv Process

The flow diagram of the acetosolv process is sketched in Figure 2.3 and a photo of the setup is supplied in the Appendix (Figure A.6). The reaction solvent, or acetosolv mix, was a 70 wt.% mixture of aqueous acetic acid. In a typical batch, 0.5 kg was combined with 3.5 L of acetosolv mix in a 4 L stirred reactor that was heated to 110 ºC. Once heated, 15 mL of an acid catalyst (H_2SO_4) was added. The temperature was held for 1 h with reflux and agitation such that the corn residues were macerated into a slurry. Upon completion, the reactor contents were vacuum filtered with 100 mesh polypropylene. The pulp retentate was recombined with 3.5 L of acetosolv mix to wash off any more residues then filtered again. Once more, the pulp was washed with 3.5 L of ethanol and filtered. The liquid filtrates of all three washes were combined then passed through a

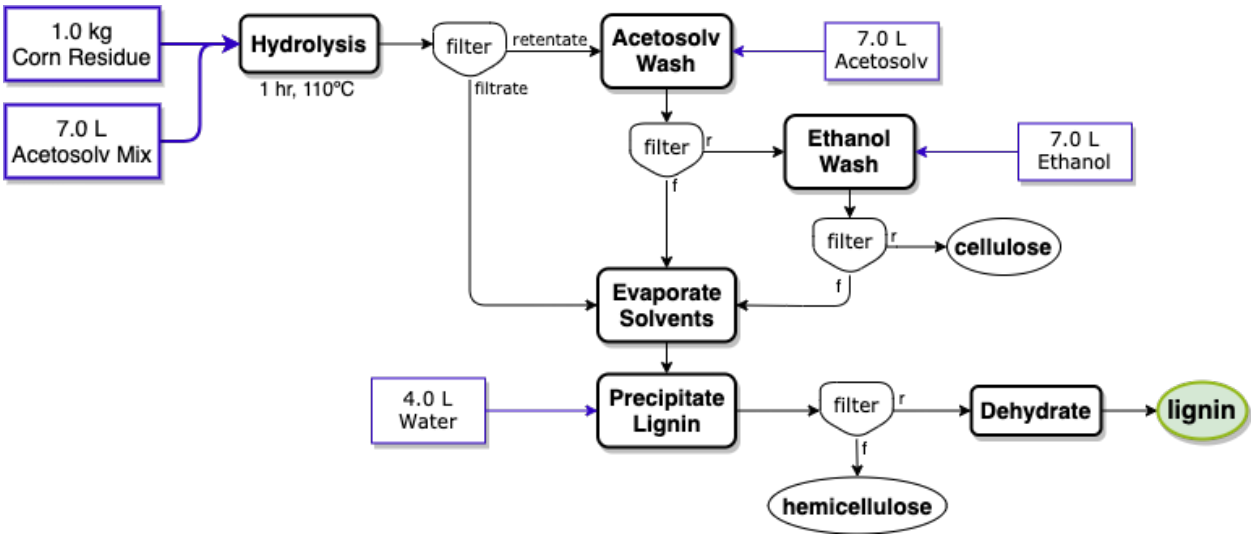

Figure 2.3: Diagram of acetosolv process developed for lab-scale fractionation of corn residues.

20 micron filter. The filtrate's solvents were evaporated to ca. 60% solids creating a highly viscous extract. Upon the addition of water (2.0 L), lignin precipitates from the extract while hemicellulose remains in solution. The cellulosic pulp and lignin solids were then dried and analyzed.

2.2.3 Characterization of Extracted Lignins

Techniques for characterization are briefly reported below and fully detailed in Appendix A.3.

Elemental (CHNO) Analysis

Elemental composition was measured using approximately 200 mg samples of lignin in two separate analyses. Measurements of CHN were collected using an Elementar Max Cube elemental analyzer. The extractive contents (i.e., Al, B, Ca, Co, Cr, Cu, Fe, K, Mg, Mn, Mo, Na, Ni, P, S, and Zn) were measured via Inductively Coupled Plasma (ICP) with a Spectro Arcos ICP-OES analyzer. Oxygen content was then determined by the remainder of composition.

Gel-Permeation Chromatography (GPC)

GPC analysis was conducted with an Agilent 1260 Infiniti system equipped with a 300mm Polargel-M and 300mm Polargel-L in series. Dried samples of lignin (approximately 40 mg) were dissolved 1.0 mL of dimethylformamide (DMF) for GPC analysis. Spectra were collected using a refractive index detector as the samples eluted in a mobile phase of DMF at 40 ºC.

^{1}H-^{13}C Heteronuclear Single Quantum Coherence (HSQC) NMR

Lignin samples of approximately 100 mg were dissolved in dimethylsulfoxide-d_6 (DMSO) for 2D solution state NMR. A 500 MHz Bruker AVIII spectrometer equipped with a multinuclear BFFO cryoprobe was used for analysis. ^{1}H and ^{13}C spectra were collected via HSQC NMR using the hsqcedetqpsisp2.2 program. Further details are provided in Appendix A.3.3.

2.3 Results & Discussion

2.3.1 Lignin Yield

Lignin was successfully extracted from corn stover (not shown) and corn cobs (Table 2.1). The recovery of lignin ranged from 14.1-17.0 wt.% of the initial mass. Fluctuations were due to random experimental errors and inconsistencies in the biomass. The average recovery of 15.1 wt.% agrees with reported yields in other literature (Kumar and Sharma, 2017; Woźniak et al., 2021)

Table 2.1: Recoveries of cellulosic pulp and lignin from acetosolv processing of corn cobs.

Batch	Pulp Recovery (wt.%)	Lignin Recovery (wt.%)
1	48.9	15.1
2	47.7	14.2
3	49.3	17.0
4	47.7	14.1
5	50.6	15.8
6	45.1	16.9
average	48.2 ± 1.9	15.1 ± 1.2

2.3.2 CHNO Elemental Analysis

For comparison with commercially sourced lignin, elemental analysis was performed on the commercial lignin samples (SL1 and CL1) and a lignin sample extracted in this work (CL2). According to Table 2.2, the compositions of lignin extracted from corn stover (SL1) and corn cobs (CL1 and CL2) are noticeably different. Corn cobs and stover serve visibly different functions to

Table 2.2: Elemental composition of acetosolv lignin samples extracted from corn cobs and stover.

Sample	C (%)	H (%)	N (%)	O[a] (%)	Other[b] (%)
SL1	59.01	5.67	1.85	32.92	0.56
CL1	55.44	4.15	0.39	39.03	0.99
CL2	54.73	4.37	0.57	39.38	0.95

[a] Calculated based on 100% less C%, H%, N%, Extractives %

[b] Elements heavier than Na and detectable by ICP

the plant, hence this difference is not unexpected. While the disparity in CHNO contents between the different sources of corn cobs (CL1 and CL2) is minimal, the disparity between the corn cobs and stover (SL1) is likely caused by disproportionate structural motifs rather than fundamentally distinct macrostructures. Based upon these results, the process demonstrated in this work can reliably produce lignins identical in quality to commercially extracted acetosolv lignins.

2.3.3 Molecular Weight Distribution

Each lignin sample's molecular weight distribution was conducted via GPC analysis. Chromatograms of stover lignin (SL1) and cob lignin (CL1) are overlaid in Figure 2.4. As can be inferred by the two near-congruent curves, the lignin samples are qualitatively similar in molecular weight distribution which reveals a similar extent of depolymerization during extraction. Quantita-

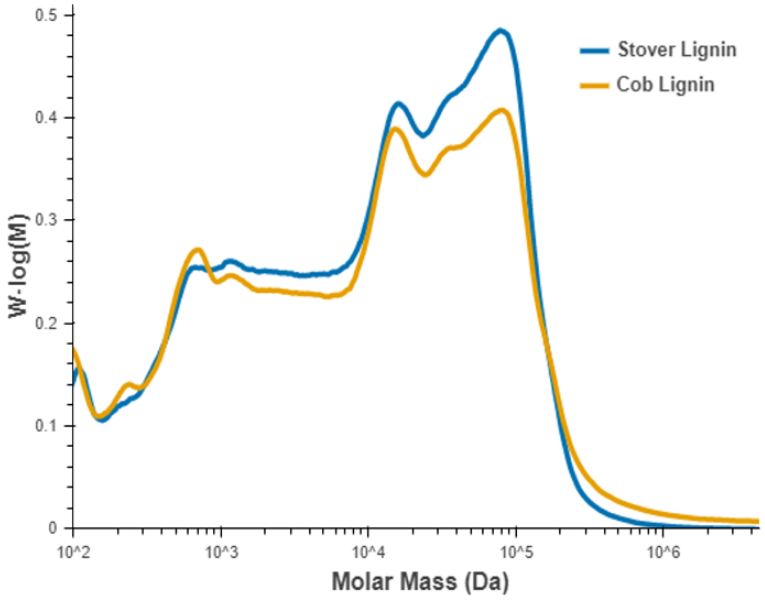

Figure 2.4: GPC spectrogram for lignin derived from corn stover (SL1) and corn cobs (CL1).

tive differences between the two lignins are apparent above 10^4 Da (relative to PMMA). However, the nearly identical curvature of the chromatograms suggests that the macrostructures share much of the same connectivity. In combination with the elemental measurements (Table 2.2), these findings suggest that SL and CL lignins are structurally similar despite observed differences in content across the molecular weight distribution.

2.3.4 Structural Analysis via HSQC NMR

To obtain a deeper understanding of the molecular connectivity of lignin after acetosolv extraction, samples of SL and CL were analyzed using two-dimensional ^{1}H-^{13}C HSQC NMR. In the aromatic region of the HSQC spectra (Figure 2.5), the functionality of the phenylpropanoid sidechains and relative H/G/S structures are apparent. Qualitatively, the regions are nearly identical which supports the findings from CHNO and GPC analyses. The peaks at $\delta H/\delta C$ 7.33/111.0 and $\delta H/\delta C$ 7.11/123.3 are present in evidential quantities for both samples. These peaks represent the signals of C_2 and C_6 in the ferulic acid (FA) motif which is of notable interest. Several peaks associated with the *p*-coumaric acid (*p*CA) motif are also apparent for both lignins. This is in agreement with multiple studies that report the presence of FA at 1-3 wt.% and *p*CA at 4-8 wt.% for corn residues (Wen et al., 2012; Min et al., 2014; Timokhin et al., 2020). Based upon the esti-

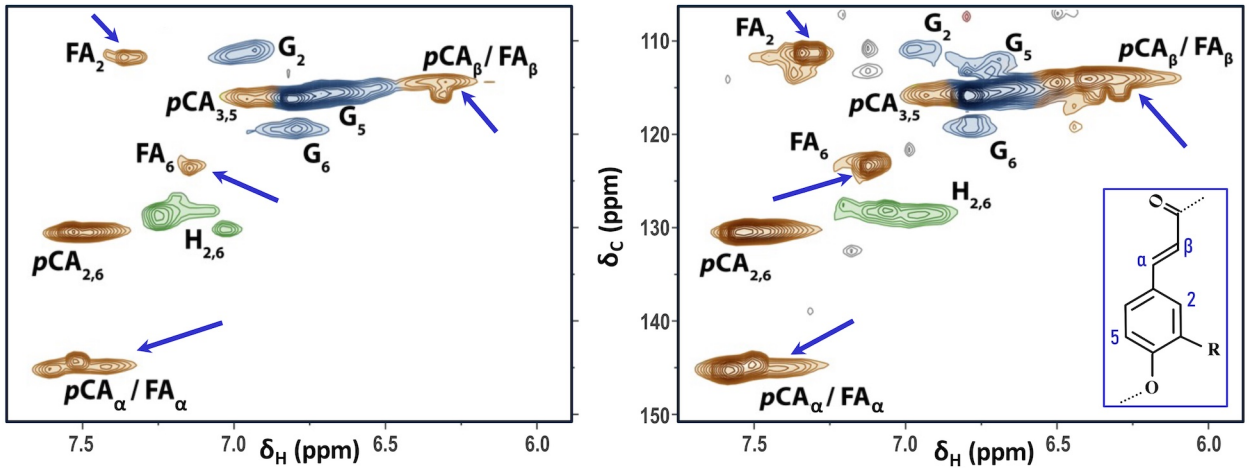

Figure 2.5: Aromatic region of ^{1}H-^{13}C HSQC NMR spectrogram for stover lignin (SL1; left) and cob lignin (CL1; right). *p*CA: *p*-coumaric acid, FA: ferulic acid, G: guaiacyl, H: hydroxyphenyl.

mated peak volumes, the lignin samples share similar ratios of H/G/S monolignols, as expected. In total, this analysis demonstrates a qualitatively identical superstructure between SL and CL with a marginal quantitative disparity.

2.4 Conclusions

Lignin was successfully extracted from corn stover and corn cobs using an industrially proven acetosolv process that allows high throughput. We demonstrated a large lab-scale procedure capable of processing corn residues at 0.5 kg/h in a simple stirred reactor. Corn cobs produced an average of 15.1 wt.% of lignin which is in agreement with other published work. Compared to corn cob lignin samples produced by ADM, those generated in this work are nearly identical in elemental contents. When comparing stover lignin to cob lignin, their elemental compositions were appreciably different. However, structural analyses via ^{1}H-^{13}C HSQC and GPC revealed that the disparity is due to differences in the contents of structural motifs rather than a fundamentally different macrostructure. The HSQC spectra of stover lignin and cob lignin are qualitatively identical in the aromatic side-chain regions and GPC showed a highly similar molecular weight distribution.

The demonstrated acetosolv process that uses environmentally friendly and food-safe solvents should also be applicable for separating cellulosic and lignin fractions from other emerging feedstocks such as wheat straw, sorghum, sugarcane bagasse, and bamboo. Due to minimal degradation of the individual fractions, the acetosolv process is well-positioned to facilitate valorization of all the biomass fractions. Demonstration of this scaled-up approach was critical to the development of commercially viable technologies for the valorization of lignin from corn residues, as explained in the next chapter.

Chapter 3

Continuous Spray Ozonolysis of Acetosolv Lignin: Reactor Engineering Studies

3.1 Background

Previously, spray ozonolysis of acetosolv lignin has been shown to selectively yield high-value phenolic aldehydes, vanillin and *p*-hydroxybenzaldehyde (*p*HB), at ambient temperature and pressure. Due to mild acylation in the acetosolv process, *C*=*C* linked units (i.e., ferulates and coumarates) are retained in acetosolv lignins (Jasiukaitytė-Grojzdek et al., 2020). Cleavage of these pendant *C*=*C* moieties in lignin affords vanillin and *p*HB (Figure 3.1). Coumarates and ferulates account for ca. 7-12 wt.% of lignin derived from corn residues (Min et al., 2014; Timokhin et al., 2020). The mild conditions and environmentally-benign compounds of ozonolysis make it an attractive alternative to other valorization technologies. Further, the selective release of only monomers from lignin during rapid ozonolysis promotes a much easier product separation.

In this thesis, additional detailed studies were conducted to evaluate the ability to continuously and safely operate spray ozonolysis and produce phenolic aldehydes at steady rates. Safety was evaluated on continuously monitored temperature and concentration profiles. Parametric studies

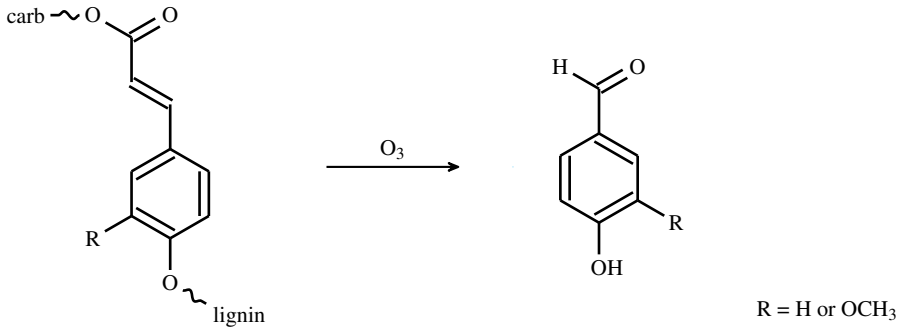

Figure 3.1: Coumarates or ferulates in lignin can be converted to phenolic aldehydes using ozone.

were used to assess the effect of inlet flow rates and feedstock concentrations on the product yields. Separate material balances for the solvent and ozone were conducted to assess how effectively these reagents are being used. Finally, versatility of the process was assessed across several sources of corn lignins. A possible correlation was hypothesized between the structural aspects of untreated lignins and the yields of vanillin and *p*HB after ozonolysis. Insights into these process aspects are essential for rational process design, optimization, and scale-up.

3.1.1 Ozonolysis Reaction Mechanism

Cleavage of the pendant coumarate or ferulate motifs follows the Criegee mechanism (Figure 3.2). During lignin extraction, cross-linked coumarate and ferulate LCCs (Figure 1.7) are partially unbound at the phenolic hydroxyl but remain terminally linked to lignin along the unsaturated side-chain. Cleavage of the *C*=*C* bond liberates the ferulate or coumarate from the lignin (Criegee, 1975). Under typical conditions, ozone attaches to the alkene via 1,3-dipolar cycloaddition forming stable but unsafe ozonide intermediates that may decompose to aldehydes. However, aldehydes may be formed directly in a suitably protic environment wherein the solvent inhibits ozonide formation by scavenging carboxyl cations (Schiaffo and Dussault, 2008; Silverman et al., 2019).

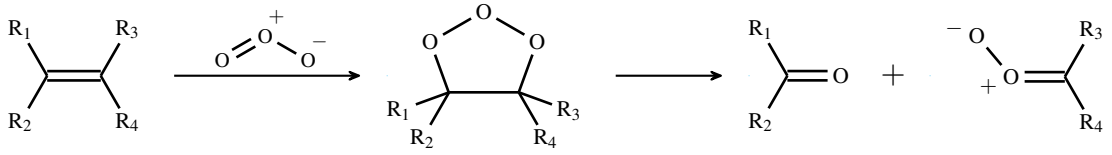

Figure 3.2: General scheme for the ozonolysis of alkene bonds as described by Criegee (1975).

3.1.2 Prior Work

We previously demonstrated the feasibility of performing ozonolysis of grass lignins in a CSTR (Danby et al., 2018) and a spray reactor (Silverman et al., 2019). For both demonstrations, ozonolysis of grass-type lignins afforded phenolic aldehydes, vanillin and *p*HB. In the CSTR, ozonolysis was hampered by long residence times that led to additional oxidation of the phenolic aldehydes. Therefore, it was hypothesized that a spray chamber could intensify production by reducing

the reliance on diffusional transport of ozone. Prior work confirmed this limitation by observing significantly higher yields using a spray mechanism during ozonolysis (Silverman et al., 2019).

3.2 Experimental

3.2.1 Re-Engineering Lignin Spray Ozonolysis

To enable systematic studies of reactor engineering, the prior experimental setup and procedure (Silverman et al., 2019) was redesigned in a new construction. Figure 3.3 details the redesigned spray ozonolysis schematic. Additional details are available in Appendix A.3.1 including a photo of the setup (Figure A.7). Notably, the redesign features a large, conical 6 L glass chamber intended to maximize contact between the spray droplets and ozone. The large chamber will facilitate future studies of scalability by employing multiple spray nozzles. To further improve the flow pattern and reduce residence time, the spray was modified for counter-current flow by relocating the nozzle to the top, opposite the ozone inlet at the bottom of the reactor. A new sampling valve at the bottom of the chamber enables a liquid seal such that the gas effluent is redirected to exit at the top. After exiting the spray chamber, the gas enters a condenser to remove entrained acid vapors that may interfere with ozone measurements. A generator from Absolute Ozone produced ozone at a dilute concentration of 1-5 mol.% in dry oxygen.

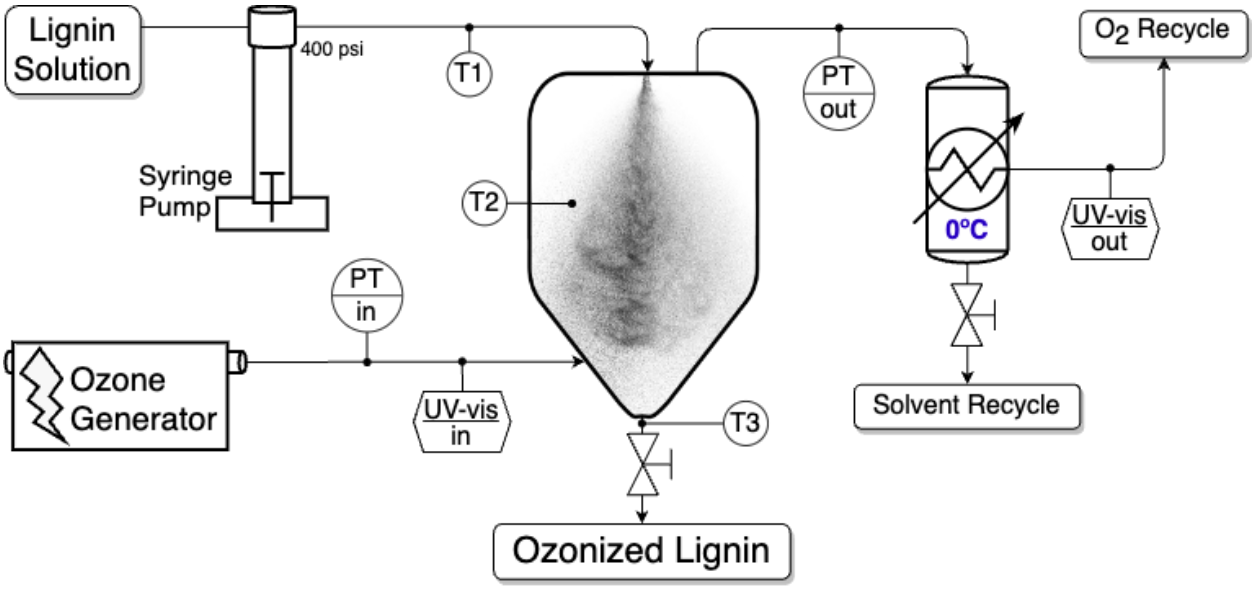

Figure 3.3: Schematic detailing the process of spray ozonolysis of lignin.

3.2.2 Process Evaluation

Reaction Monitoring

Temperature and ozone concentrations were continuously recorded during every experiment for analysis and prevention of runaway reactions. UV-vis sensors at the inlet and outlet of the spray chamber continuously profiled ozone consumption. Typically, the reaction was profiled using the average of 8 thermocouples distributed along the vertical axis parallel to the spray pattern. The exiting liquid stream was periodically sampled for product analysis.

Ozone Utilization

We define the ratio of useful consumption to total consumption of ozone (Equation 3.1) as ozone utilization ($S^*_{O_3}$). Stoichiometrically, ozonolysis consumes one mole of ozone to yield two moles of aldehydes. However, half of the aldehyde yield cannot be not quantified as it remains on the lignin macrostructure. Equation 3.1 considers only the yield of phenolic aldehydes (aryl-CHO) which represents exactly half of the reaction. Thus, $S^*_{O_3}$ should equal 1 under ideal conditions.

$$S^*_{O_3} = \frac{\text{moles } aryl-CHO \text{ produced}}{\text{moles } O_3 \text{ consumed}} \tag{3.1}$$

3.2.3 Product Analysis and Characterization

Ozonolysis product identification and quantification

Product yields are expressed as a weight percent relative to the dry mass of the lignin feedstock, as described by Equation 3.2. Gas Chromatography with Flame Ionization Detection (GC/FID) analysis identified and quantified monomers present in the ozonized product mixture against external standards. Sample preparation included the dilution of 100-300 μL of lignin solution with 1.0 mL of methanol. Analyses were carried out using an Agilent 7890A GC equipped with an HP-INNOWAX column. The oven temperature was ramped from 40 ºC to 220 ºC at 10 ºC/min. Figure 3.4 shows the GC/FID chromatogram obtained from an ozonized product. The analytical method and calibration is fully detailed in in Appendix A.3.2.

$$Y_C\ (wt.\%)\ = \frac{m_C}{m_L} * 100 \tag{3.2}$$

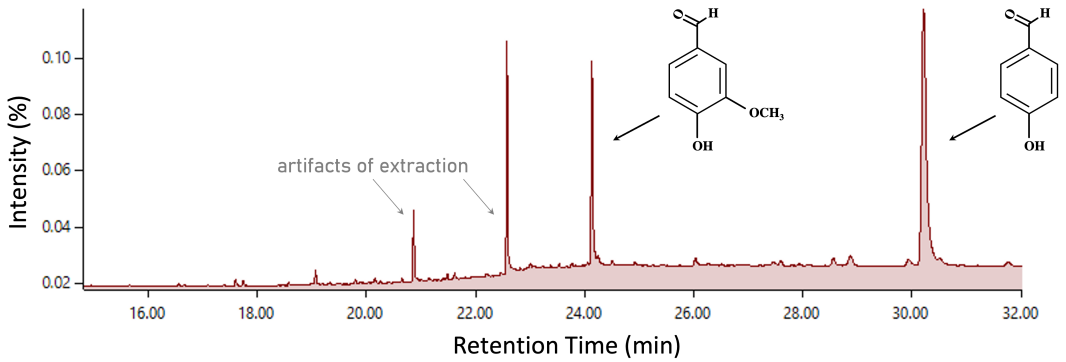

Figure 3.4: Phenolic aldehyde products, vanillin (24.14 min) and *p*HB (30.24 min), identified in the FID chromatogram of ozonized lignin (OZCL1) including monomer artifacts from extraction.

Separation of ozonolysis product mixture

For characterization, the product mixture after ozonolysis (OZL) was separated into two fractions using liquid extraction as demonstrated by Silverman et al. (2019). Shortly after ozonolysis, the reaction solvent was completely evaporated from the OZL. The dried solids were combined with ethyl acetate at 50 mL per g of lignin. Roughly half the mass of solids remained undissolved as the high molecular weight (HMW) fraction. The HMW solids were filtered from the ethyl acetate solution containing the low molecular weight (LMW) fraction of monomers and oligomers. The LMW was recovered by evaporating the ethyl acetate.

Determination of molecular size distribution

Approximately 40 mg of dried ozonized lignin samples were dissolved in 1.0 mL of DMF for GPC analysis. Chromatograms were collected via refractive index using an Agilent 1200 Infinity Series. Using a mobile phase of DMF, the lignin samples were eluted through a 300 mm Polargel-M column followed by a 300 mm Polargel-L column at 40 ºC. The resultant chromatograms are calibrated to poly(methyl methacrylate). See Appendix A.3.5 for more details.

Analyzing chemical structure of ozonized lignin

Fourier-Transform Infrared spectroscopy (FTIR) was used in conjunction with elemental analysis as described in Section 2.2.3. For FTIR, samples of the untreated lignin solution and ozonized lignin solution were dried for analysis. For each sample, approximately 5 mg was combined with 1.0 g of KBr powder, ground to a find powder, then pressed into a disc. The discs were analyzed using a Bruker Tensor T27 FTIR. More information is provided in Appendix A.3.4

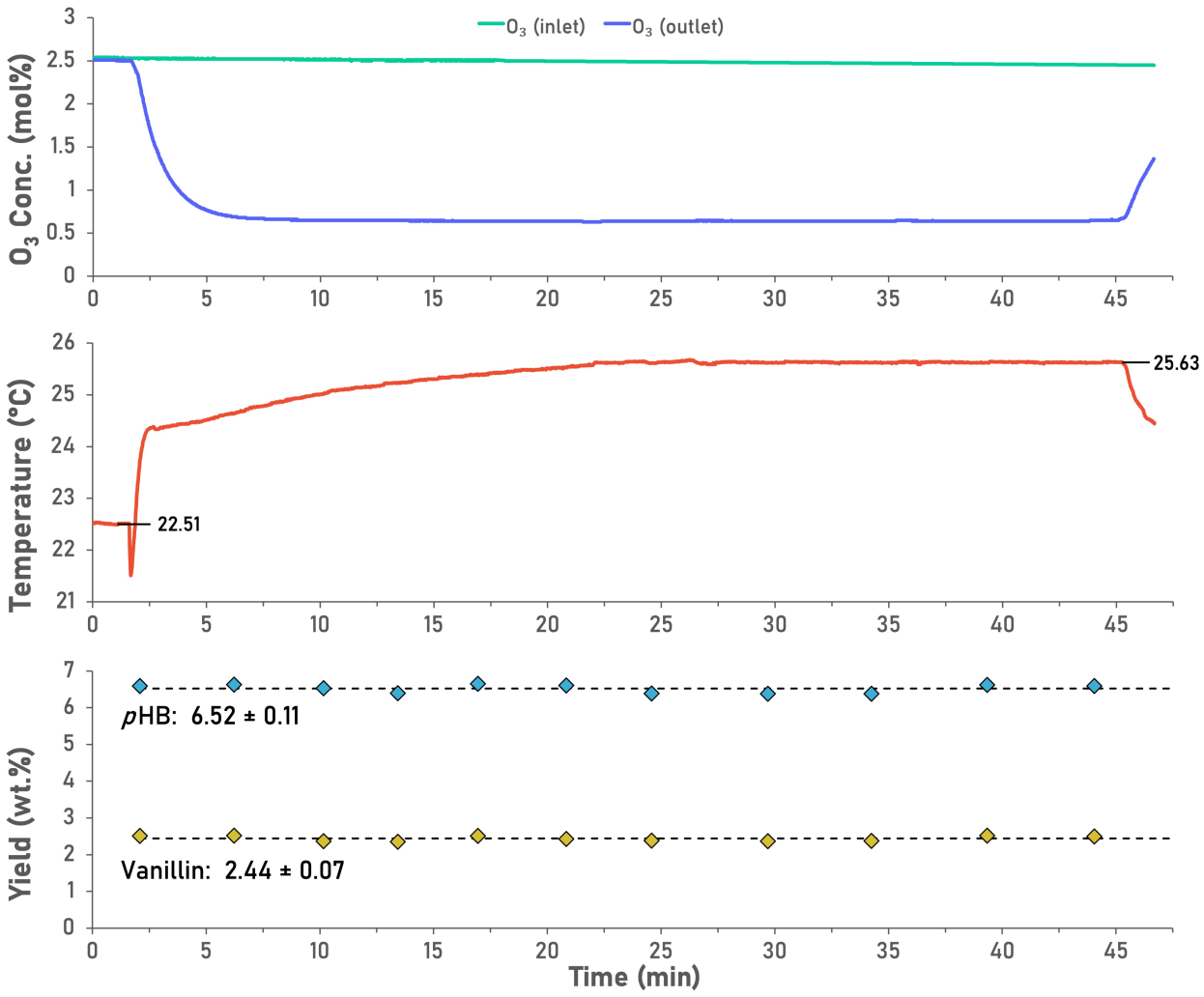

Figure 3.5: Temporal profiles recorded during continuous spray ozonolysis of CL1. Conditions: 1.0 wt.% CL1 at 4.5 LPH and 2.5 mol% O_3 at 3.0 SLPM.

3.3 Results & Discussion

3.3.1 Temporal Temperature and Ozone Consumption Profiles

Proper temperature control in the reactor is necessary to prevent thermal runaway and ensure safe operation of the exothermic ozonolysis reaction. As can be seen in the temperature profile of Figure 3.5, the measured temperature rise in the reactor during continuous operation does not exceed 5 °C including an initial spike of several degrees. The temperature profile attains a more or less stable value after nearly 30 minutes. Such a stable profile without an overshoot suggests that the solvent acts as a sink to remove the heat of reaction. Convective heat exchange between the liquid droplets and the flowing gas stream may also contribute to the mediation of temperature.

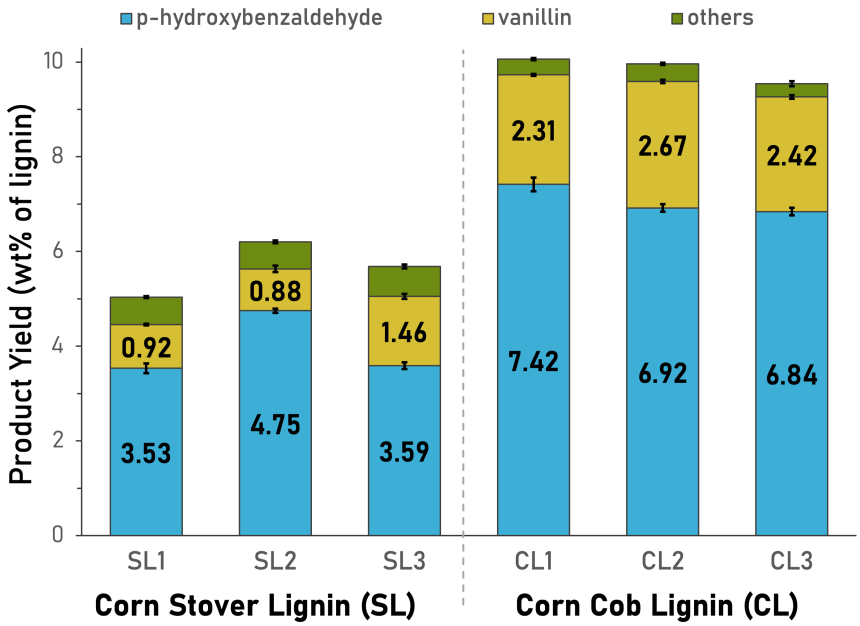

Figure 3.6: Steady-state yields of phenolic aldehydes from continuous spray ozonolysis of lignin from corn residues. Conditions: 4.5 LPH of 1.0 wt.% lignin solution sprayed into 3.0 SLPM of 2.5 mol% O_3 at ambient temperature and pressure.

The ozone concentration profile displayed in Figure 3.5 indicate a gradual decrease in ozone that plateaus near 5 min. However, the products reach steady-state yields almost immediately (10 s) after the reaction begins. The profile of product yields is also plotted in Figure 3.5. This disparity is attributed to the different dynamics of mixing in the gas phase prior to reaching a steady state. As the product yield profile reveals, steady-state production is reached quickly.

3.3.2 Production of Phenolic Aldehydes

A chromatogram of an ozonized product mixture (OZCL1) appears in Figure 3.4. Phenolic aldehyde products are detected at 24.14 min for vanillin and 30.24 min for *p*HB. The minor peaks are attributed to compounds present in the feed lignin mixture (e.g., 2-methoxy-4-vinylphenol at 22.58 min). In theory, it is possible to over-oxidize the phenolic aldehydes into their carboxylic acid analogues. However, GC/FID and /MS spectra reveal no detectable formation of over-oxidation products, suggesting the reaction follows Dussault's pathway (Schiaffo and Dussault, 2008).

As exhibited in Figure 3.6, the yields of aldehydes from corn cob lignin (CL) are approximately double compared to those achieved with stover lignin (SL) at identical operating conditions. All SL

samples (SL1, SL2, and SL3) were supplied by ADM. Combined phenolic aldehyde yields from the SLs are ca. 4-5.5 wt.% which is in agreement with prior work (Danby et al., 2018; Silverman et al., 2019). The exact source of the SL samples is unknown, but physical differences were apparent between the samples. The SL samples were received on separate occasions which may explain the variation in physical appearances and thus yields. In contrast, ozonolysis of corn cob lignin (CL1) produced phenolic aldehydes at a combined yield of ca. 10 wt.%. These results were repeatable with CLs from different sources (CL2 and CL3). The nearly-doubled yield of vanillin and *p*HB from CL compared to SL correlates with the higher content of ferulate and coumarate moieties in corn cobs compared to corn stover (Timokhin et al., 2020; Min et al., 2014). Based on reported ferulate and coumarate contents, it can be assumed that the ozonolysis of CL and SL yields near maximum quantities of *p*HB and vanillin.

3.3.3 Ozone Utilization During Spray Ozonolysis

To minimize the operating costs of an ozonolysis process, the useful consumption of ozone to produce phenolic aldehydes must be maximized to avoid either ozone decomposition or ozone consumption via undesired pathways. Figure 3.7 shows that ozone utilization is far less than 1 for both SL and CL ozonolysis. Interestingly, ozone utilization is approximately twice as much

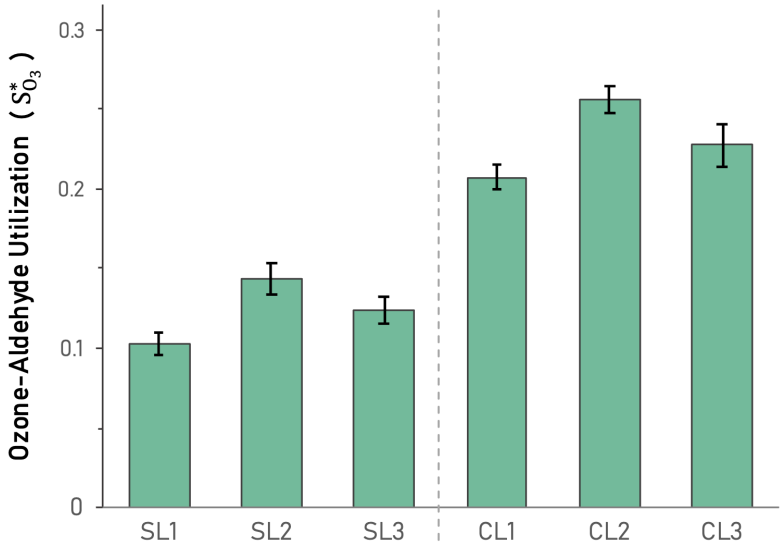

Figure 3.7: Ozone utilization during spray ozonolysis of various lignin sources where utilization is expressed as moles of produced aldehyde per moles of consumed ozone.

greater with CL compared to SL. This trend suggests that the ozone is utilized in ways other than simply severing the *C*=*C* bonds, which occurs at a twofold higher concentration in the case of CL. However, no other products are detected by GC/FID or /MS that may explain the unaccounted consumption of ozone. Blank spray runs with ozone and different neat solvents without dissolved lignin (Appendix A.4) indicate that ozone decomposition is negligible at reaction conditions.

The pathway via which the unaccounted for ozone is consumed is still unclear. It is possible that ozone could be functionalizing the aliphatic bonds in the macrostructure of lignin. Free radicals produced during ozonolysis or localized heat generation could also facilitate ozone decomposition which would not be observed in the blank experiments. Additional studies are needed to identify the cause of the excess ozone consumption.

3.3.4 Ozonolysis Minimally Alters the Elemental Composition of Lignin

Untreated CL, ozonized CL, and fractionated ozonized products were analyzed for their content of C, H, N, O and other elements which is given in Table 3.1. As is expected with ozonolysis, the treated lignin sample (OZCL1) possessed a larger concentration of oxygen at 40.98% compared to 39.03% before treatment. Assuming CL1 possesses 7.5 wt.% coumarates and 2.5 wt.% ferulates, the formation of two aldehydes per *C*=*C* bond adds 1.72 g of O_2 per 100 g of lignin (see Appendix A.6 for calculations). Accounting for an increase in total mass, the adjusted O% is 40.06%. The unaccounted 0.92% of oxygen and changes in C% and H% are significant due to the reported instrument error of <0.1%. Because ozonolysis does not introduce hydrogen, the solvent

Table 3.1: Elemental composition of untreated and ozonized samples of lignin from corn cobs.

Sample	**C (%)**	**H (%)**	**N (%)**	**O[a] (%)**	**Other[b] (%)**
CL1	55.44	4.15	0.39	39.03	0.99
OZCL1	52.23	5.25	0.56	40.98	0.99
HMW-OZCL1	46.33	5.05	1.55	44.29	2.78
LMW-OZCL1	43.22	5.30	0.15	51.12	0.20

[a] Calculated based on 100% less C%, H%, N%, Extractives%

[b] Elements heavier than Na and detectable by ICP

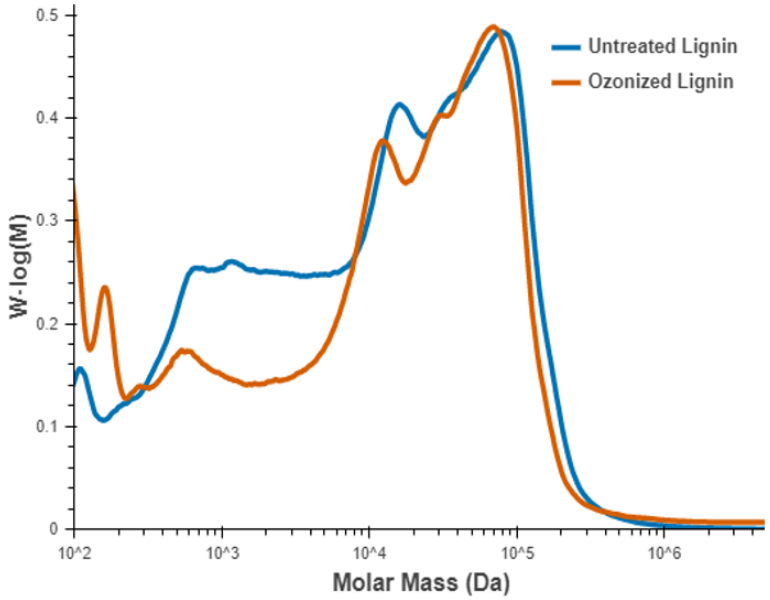

Figure 3.8: GPC spectra for untreated corn cob lignin (blue) and ozonized cob lignin (orange).

may be interacting with lignin. The acetic and formic acid mixture may induce hydroxylation of lignin which could partly account for both the increase in H% and unaccounted O%. Further investigation including a full analysis of the fractionated products (HMW-OZCL1 and LMW-OZCL1) is required to determine this relationship.

3.3.5 Molecular Weight Distribution of Ozonized Lignin

GPC analysis of the ozone-treated lignin (Figure 3.8) reveals a decrease in the molecular weight distribution corresponding to a reduction in complexity. There is a significant decrease in polymer units between 10^3-10^4 Da which may be the result of depolymerization that occurs when the $C{=}C$ bonds are cleaved by ozone. The peaks at the low-end (ca. 10^2 Da) are representative of the newly-formed monomers. Notably, the distribution curves above 10^4 Da are nearly indiscernible between the two samples. Thus, the macrostructure of ozonized lignin is largely unmarred.

3.3.6 Functionality of Ozonized Lignin

Fourier Transform Infrared (FTIR) spectra (Figure 3.9) were collected for several samples including the untreated CL (CL3) and ozone-treated CL (OZCL3). Typical of lignin, there's a broad

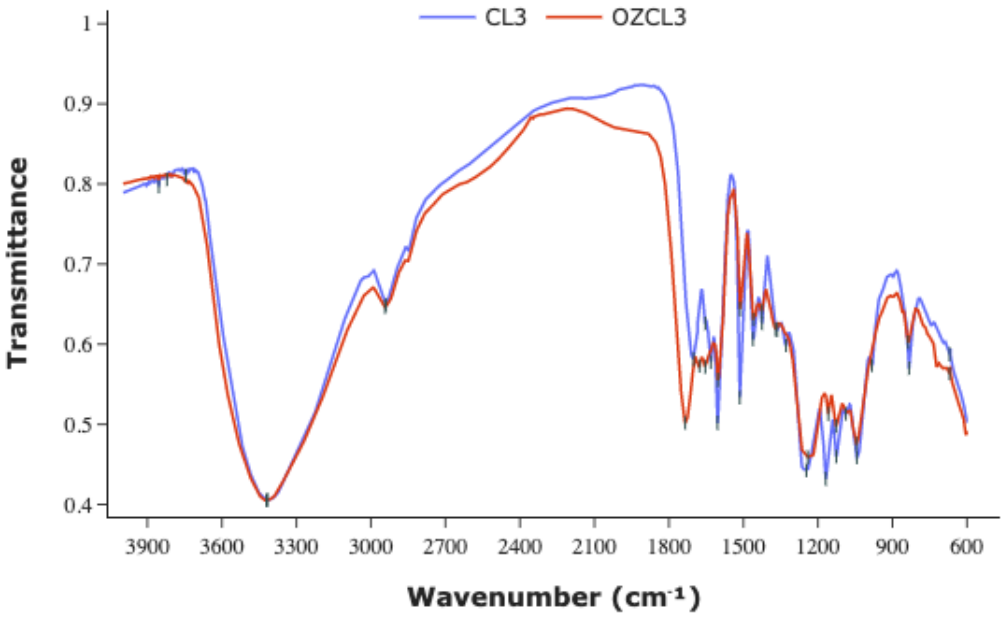

Figure 3.9: FTIR spectra of untreated (CL3; blue) and ozonized (OZCL3; red) cob lignin samples.

hydroxyl band at 3409 cm^{-1} which does not appear to be affected by ozonolysis. The peak at 1733 cm^{-1} is assigned to unconjugated $C{=}O$ stretch. Skeletal vibrations of monolignols (H/G/S) are assigned to the peaks at 1603 and 1514 cm^{-1}. The reduction of the skeletal vibrations of the monolignols and the increase in unconjugated $C{=}O$ stretch suggests the formation of phenolic aldehydes from the phenolic monolignols. OZCL3 does not appear to possess additional functionality to any significant degree that would support the hypothesis that excess ozone may be functionalizing lignin's macrostructure.

3.4 Parametric Studies of Spray Ozonolysis Reactor

Parametric studies of four process variables were conducted to investigate the dynamics of ozonolysis in a spray chamber. The variables were ozone concentration, gas flow rate, liquid flow rate, and solvent composition. All studies were compared to a baseline experiment using conditions identical to those in Figure 3.6 which are also listed in Table 3.2, unless otherwise specified. The correlations discovered in these experiments will guide a rational optimization of the spray ozonolysis process in future work.

Table 3.2: Baseline process conditions lignin ozonolysis.

Parameter	Gas Stream	Liquid Stream
Solute concentration	2.5 mol% O_3	1.0 wt.% lignin
Solvent	oxygen	3:1 AcOH:FmOH [a]
Total flow rate	3.0 SLPM	4.5 LPH
Temperature	ambient ± 5°C	
Pressure	ambient ± 4 psi	

[a] 3:1 v/v of glacial acetic acid to 88% formic acid

3.4.1 Effects of Flow Rates and Ozone Concentration

Feed flow rates affect product yields dictated by the physics of spray nozzles. At low liquid flow rates, the dispersion capacity of the nozzle is severely diminished. This effect is nominal at sufficiently high flow rates (Cerruto et al., 2021). It is also likely that the high gas flow rates can influences the spray dispersion. Experimental flow rates of liquid and gas streams were chosen within the well-dispersed regime where these effects are minimal. Droplet size is similarly influenced by liquid flow rate, but the effect is likely limited over the flow ranges (Cerruto et al., 2021). Both flow rates impact the contact time between ozone and the droplets.

Liquid Flow Rate

Figure 3.10a indicates that liquid flow rate is inversely proportional to yield. Because the contact time decreases with increased flow rate, this result is expected. The flow dynamics of the spray dictates droplet coalescence and therefore causes variations in contact area and time between the liquid and gas phases. A systematic study of the effect of liquid flow rate on nozzle flow dynamics is needed to better understand the observed effects.

Gas Flow Rate

Figure 3.10b reveals that yields increase with gas flow rate, reaching a maximum at 3.0 SLPM. Whereas ozone concentration was held constant at 2.5 mol%, ozone throughput increased as dictated by the combined gas flow rate. In Figure 3.10b, ozone throughput rises left-to-right (30, 48, 75, and 90 SCCM). Below 3.0 SLPM, the product yields are likely starved of ozone. Above 3.0 SLPM, product yields are likely limited by contact time between the liquid and gas phases.

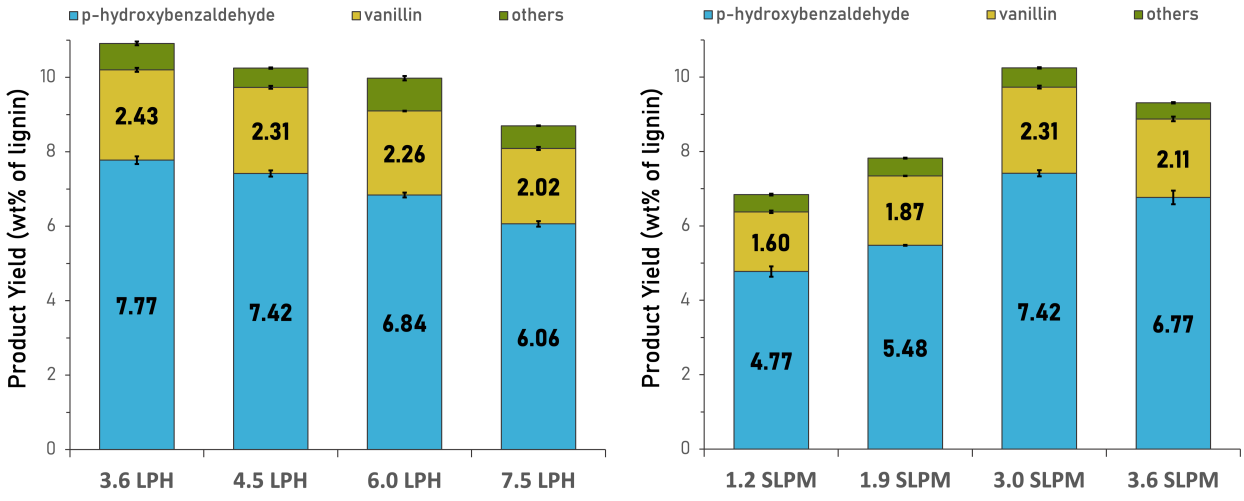

(a) Liquid Flow Rate

(b) Gas Flow Rate

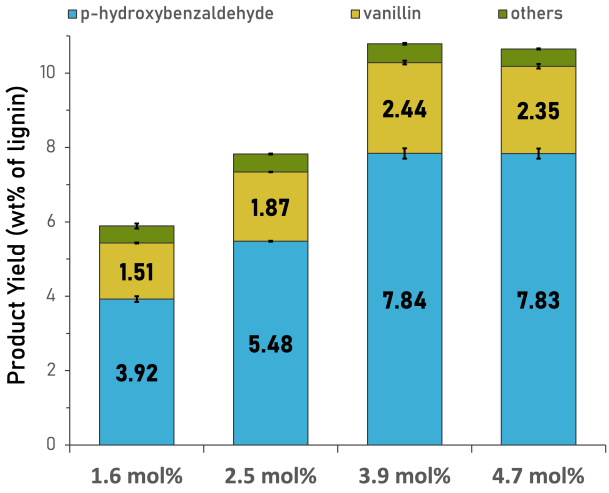

(c) Ozone Concentration

Figure 3.10: Investigations of the indicated parameters effect on the steady-state yields of phenolic aldehydes during spray ozonolysis of CL1. Conditions are listed in Table 3.2 except as noted.

Ozone Concentration

Due to constraints imposed by the ozone generator, investigation of ozone concentration employed a gas flow rate of 1.9 SLPM compared to the 3.0 SLPM baseline. Therefore, the yields of the run indicated at 2.5 mol% in Figure 3.10c are lower than the baseline. For reference, the 2.5 mol% run in Figure 3.10c is equivalent to the 1.9 SLPM experiment in Figure 3.10b.

Based upon the trend in Figure 3.10c, ozone concentration is directly correlated to phenolic aldehyde yield. This may suggest that the ozonolysis reaction to produce the phenolic aldehydes may be limited by diffusion rates causing ozone starvation within the droplets. Higher ozone

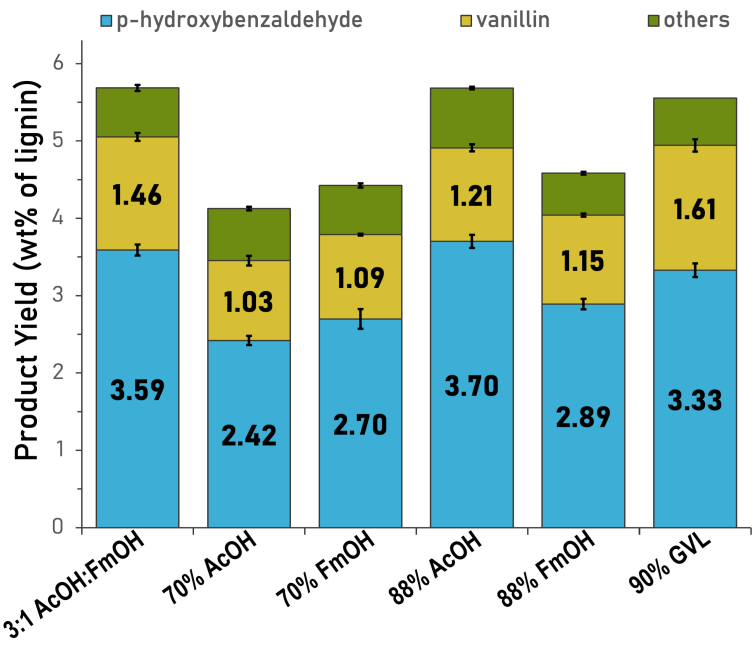

Figure 3.11: Effect of various solvents on the steady-state yields of phenolic aldehydes during spray ozonolysis of SL3. Conditions are listed in Table 3.2, except solvent as indicated.

concentrations increase diffusion rates and thereby alleviate ozone starvation. This explanation is also consistent with the increased yield at higher gas flow rates (Figure 3.10c).

3.4.2 Solvent Effects

An evaluation of several solvents was performed to discover insights into the solvent's role in yielding phenolic aldehydes and the solvent's ability to sufficiently dissolve lignin. Only a few solvent combinations with the required solvent properties are accessible to overcome the generally poor solubility of lignin. Mixtures of water with acetic acid (AcOH), formic acid (FmOH), and γ-valerolactone (GVL) were explored. This experiment examined yields from stover lignin samples (SL3), but the results should apply to cob lignin as well.

As can be seen in Figure 3.11, solvent selection had a marked effect on yields. Compared to the baseline mixture (3:1 AcOH:FmOH), the other solvents underperformed. Despite obtaining similar combined yields with 88% AcOH and 90% GVL, both solvents may be less practical than the baseline. While GVL is a greener solvent, it is not yet commercially viable. In contrast, a binary mixture like 88% AcOH may be more commercially desirable than the ternary baseline

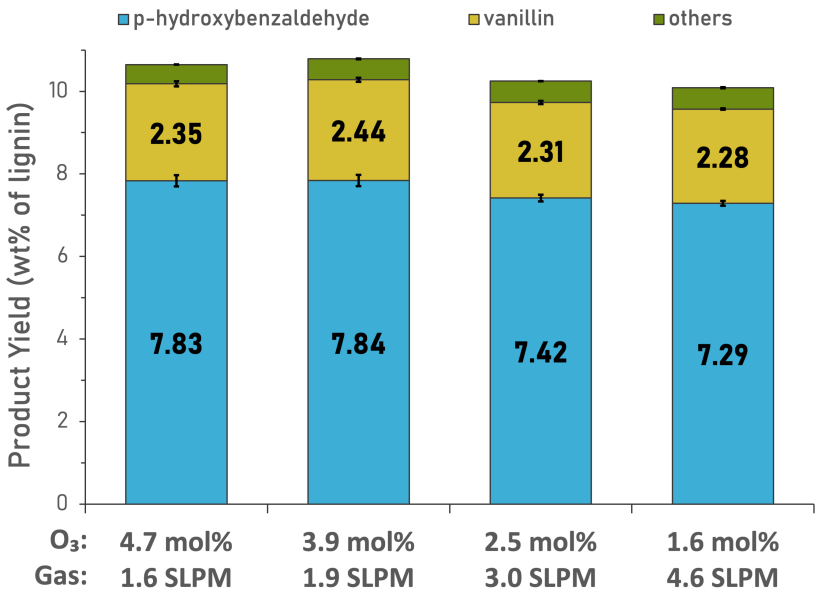

Figure 3.12: Combined effect of ozone concentration and total gas flow rate on the steady-state yields of phenolic aldehydes during spray ozonolysis of CL1. Ozone throughput was held constant at 75 SCCM for each run. Conditions are listed in Table 3.2, except as indicated.

mixture. However, this solvent may limit solubility at higher lignin concentrations (>3 wt.%).

The role of the solvent beyond scavenging free radicals during ozonolysis is still unclear. Viscosity and proticity have a larger role than can be determined from these preliminary studies. Hansen solubility parameters may better inform the role of solvent properties in facilitating phenolic aldehyde production (Novo and Curvelo, 2019). Future work will explore these concepts on a broader spectrum of solvents.

3.4.3 Combined Effect of Ozone Concentration and Gas Flow Rate

In this experiment, ozone concentration and total gas flow rate were varied while maintaining ozone throughput at 75 SCCM. Figure 3.12 shows that the yields amongst these runs were nearly equivalent. This trend again suggests that the overall production of the aldehydes may be governed by gas-liquid mass transfer rates, dictated by the product of the gas-liquid mass transfer coefficient and the ozone concentration gradient between the bulk gas phase and the gas-liquid surface. At lower gas flow rates, the higher ozone concentration gradient compensates for the lower mass transfer coefficient, and vice-versa. To test this hypothesis further, we carried out an experiment

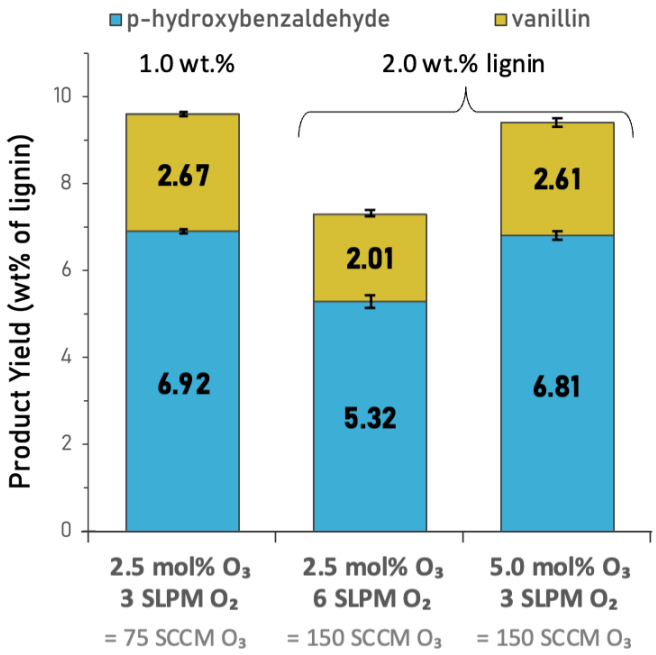

Figure 3.13: Steady-state yields of phenolic aldehydes during spray ozonolysis when doubling lignin throughput in different gas phase dynamics at constant ozone throughput. Conditions are listed in Table 3.2, except as O_3 concentration and gas flow rate as indicated.

wherein we doubled the lignin concentration in the feed solution as well the ozone concentration without changing the flow rates of the two streams (Figure 3.13). The result was a near-doubling of the total production rate of vanillin and *p*HB, confirming that the fast ozonolysis rate is dictated by the ozone diffusion rate into the droplets. In contrast, when the ozone throughput was increased by doubling the gas flow rate while maintaining an identical ozone concentration in the feed, the vanillin production rate instead dropped by approximately 25%. It is possible that the higher flow rates also affected the spray pattern and therefore the gas-liquid contacting pattern. Systematic investigations are needed to maximize vanillin production rates while maintaining safe ozone concentrations and maximizing its utilization.

3.5 Conclusions

A continuous, single-nozzle, spray ozonolysis reactor was constructed and demonstrated to selectively produce vanillin and *p*HB from lignin. An acetic-acid based lignin solution is sprayed and contacted against counter-current stream of ozone ambient temperature and pressure to effect

the ozonolysis reaction. The system reaches steady-state production of vanillin and *p*HB in 10 s or less with stable temperature control and steady ozone consumption over a run duration of nearly an hour. The cumulative product yield of vanillin and *p*HB is up to 10 wt% of the lignin feed in the case of corn cob lignin, which is nearly double the value reported previously with corn stover lignin. The overall materials balance based on the recovered solvent and product streams is >95%. However, the ozone utilization towards the desired products is only 20-25% in most cases. Parametric studies reveal that the fast ozonolysis process is controlled by gas-liquid mass transfer rates, providing valuable guidance for resource-efficient process design and scale-up.

Chapter 4

Future Prospects

Despite favorable results, demonstrating commercial viability of the proposed acetosolv extraction and ozonolysis technologies will require additional studies. The following is a discussion of research prospects and recommendations for the future of this work.

4.1 Improvements to Lignin Extraction

Industrial equipment to reduce operating costs

Acetosolv extraction, as constructed, possesses minimal operational complexity to the detriment of material and energy inefficiencies. Such simplistic batch extractions required solvent volumes in excess of 7 L per kg of biomass during hydrolysis. Regardless of recycling capability, energy costs of solvent recycling may be overwhelming. Instead, implementing industrial equipment is recommended to reduce the solvent and energy demands in a continuous capacity.

Screw-type processing units, employed in wastewater, pharmaceutical, and polymer industries,

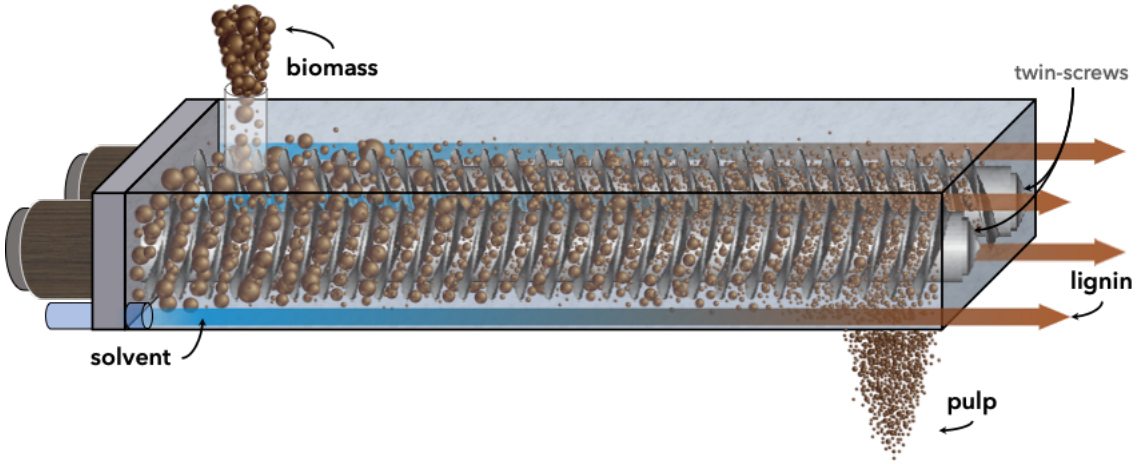

Figure 4.1: Twin-screw biomass extractor concept based on existing twin-screw granulation units.

can be made suitable for lignin extraction with minor modifications (Seem et al., 2015). The envisioned unit (Figure 4.1) feeds the biomass and solvent into a heated chamber with a twin-screw mechanism to continuously macerate the biomass and extract the lignin as the biomass moves through the chamber. In this manner, the high shear rate improves mixing thus reduces the necessary solvent volume. In combination with the expertise of Binder and Hagberg (2020), the twin-screw reactor is estimated to require as little as 4 L per kg of biomass.

Screening Emerging Feedstocks

Several sources of biomass, similar to corn residues, are noted as emerging feedstocks in the future bioeconomy. Sources may include wheat, sorghum, sugarcane, miscanthus, and bamboo. A method to screen feedstocks for their potential yield of phenolic aldehydes is necessary to alleviate the substantial barriers of evaluating the biomass in-situ. Analyzing CL and SL with ^{1}H-^{13}C HSQC NMR (Section 2.3.4) revealed that structural composition of the lignins may correlate with the yield of phenolic aldehydes in spray ozonolysis. Future investigations should evaluate the viability of such a method to screen biomass feedstocks for their valorization potential.

4.2 Improvements to Spray Ozonolysis of Lignin

Increased Lignin Throughput

Recommendations to improve the throughput of lignin ozonolysis are two fold: (1) scale out of spray capacity and (2) scale-up of lignin concentration. The throughput of lignin scales linearly with either parameter. The spray capacity can be scaled out via the addition of multiple nozzles per chamber and multiple chambers in parallel. Increasing the concentration of lignin beyond 1.0 wt.% would easily improve throughput, but the solubility of lignin is of concern for concentrations higher than 5.0 wt.%. A rational scale-up should be devised to accommodate both changes.

Alternative Solvents

Preliminary screening experiments for ozonolysis revealed that the solvent had a clear impact on the phenolic aldehyde yields. Future experiments should evaluate alternative solvents for their capacity to dissolve higher concentrations of the acetosolv lignin and their ability to limit formation

of ozonide intermediates. Potential candidates are likely to be ternary mixtures, but future work should prioritize pure or binary solvents for sake of commercial viability.

Product Separation Schemes

We envision the maximum value of the phenolic aldehydes will be realized through individual product streams. Thus, a scheme to systematically separate vanillin and *p*HB from the ozonolysis product mixture must be devised. Foremost, the separation must be scalable and economically viable. Initial separation of the low and high molecular weight fractions was demonstrated in this and prior work (Silverman et al., 2019). The vanillin and *p*HB must be isolated from the low molecular weight fraction. We proposed chromatography for the selective separation of vanillin and *p*HB followed by a supercritical-fluid antisolvent (SAS) process for the purification and crystallization of the individual product streams, as recently demonstrated (Kinn, 2022). Despite limited industry adoption, chromatography may be commercially viable as a continuous process using a simulated moved bed. However, SAS crystallization is well established in the pharmaceutical industry (Subramaniam et al., 2000; Snavely et al., 2002). Future work will evaluate practical separation methods using a combination of SAS crystallization and chromatographic separation.

4.3 Technoeconomic Assessment of a Modular Biorefinery

In traditional agricultural processing, acquisition and treatment of the biomass often accounts for up to 50% of operating costs (Den et al., 2018). Thus, we propose the agricultural processing and lignocellulose valorization of biorefineries should be distributed around the supply of biomass. For the proposed technologies, the equipment may be built in a modular manner whereby scale is achieved through a simple scale-out approach. In such a manner, the processing facility may be brought to the biomass supply (i.e., distributed manufacturing), therefore reducing logistics and procurement costs. Hence, we recommend to conduct a technoeconomic assessment of the valorization of corn residues in a decentralized biorefinery using acetosolv extraction and spray ozonolysis. Assessment will include process simulations using experimental data to identify bottlenecks and guide development.

References

Langan, P. et al. (2014) Common processes drive the thermochemical pretreatment of lignocellulosic biomass. *Green Chem. 16*, 63–68.

Spiridon, I., and Popa, V. I. In *Monomers, Polymers and Composites from Renewable Resources*; Belgacem, M. N., and Gandini, A., Eds.; Elsevier: Amsterdam, 2008; pp 289–304.

Kumar, A. K., and Sharma, S. (2017) Recent updates on different methods of pretreatment of lignocellulosic feedstocks: a review. *Bioresources and Bioprocessing 4*.

Jasiukaitytė-Grojzdek, E., Huš, M., Grilc, M., and Likozar, B. (2020) Acid-catalysed α-O-4 aryl-ether bond cleavage in methanol/(aqueous) ethanol: understanding depolymerisation of a lignin model compound during organosolv pretreatment. *Scientific Reports 10*, 11037.

Tarasov, D., Leitch, M., and Fatehi, P. (2018) Lignin–carbohydrate complexes: properties, applications, analyses, and methods of extraction: a review. *Biotechnology for Biofuels 11*.

Hocking, M. B. (1997) Vanillin: Synthetic Flavoring from Spent Sulfite Liquor. *Journal of Chemical Education 74*, 1055.

Upton, B. M., and Kasko, A. M. (2016) Strategies for the Conversion of Lignin to High-Value Polymeric Materials: Review and Perspective. *Chemical Reviews 116*, 2275–2306.

Criegee, R. (1975) Mechanism of Ozonolysis. *Angew. Chem., Int. Ed. 14*, 745–752.

Azadi, P., Inderwildi, O. R., Farnood, R., and King, D. A. (2013) Liquid fuels, hydrogen and chemicals from lignin: A critical review. *Renewable and Sustainable Energy Reviews 21*, 506–523.

Tocco, D., Carucci, C., Monduzzi, M., Salis, A., and Sanjust, E. (2021) Recent Developments in the Delignification and Exploitation of Grass Lignocellulosic Biomass. *ACS Sustainable Chemistry & Engineering 9*, 2412–2432.

Wei Kit Chin, D., Lim, S., Pang, Y. L., and Lam, M. K. (2020) Fundamental review of organosolv pretreatment and its challenges in emerging consolidated bioprocessing. *Biofuels, Bioproducts and Biorefining 14*, 808–829.

Rinaldi, R., Jastrzebski, R., Clough, M. T., Ralph, J., Kennema, M., Bruijnincx, P. C. A., and Weckhuysen, B. M. (2016) Paving the Way for Lignin Valorisation: Recent Advances in Bioengineering, Biorefining and Catalysis. *Angewandte Chemie International Edition 55*, 8164–8215.

Foroughi, F., Rezvani Ghomi, E., Morshedi Dehaghi, F., Borayek, R., and Ramakrishna, S. (2021) A Review on the Life Cycle Assessment of Cellulose: From Properties to the Potential of Making It a Low Carbon Material. *Materials 14*.

McMillan, J. D. *Enzymatic Conversion of Biomass for Fuels Production*; American Chemical Society, 1994; Chapter 15, pp 292–324.

Den, W., Sharma, V. K., Lee, M., Nadadur, G., and Varma, R. S. (2018) Lignocellulosic Biomass Transformations via Greener Oxidative Pretreatment Processes: Access to Energy and Value-Added Chemicals. *Frontiers in chemistry 6*, 141.

Klemm, D., Philipp, B., Heinze, T., Heinze, U., and Wagenknecht, W. *Comprehensive Cellulose Chemistry*; John Wiley & Sons, Ltd, 1998.

Hendriks, A., and Zeeman, G. (2009) Pretreatments to enhance the digestibility of lignocellulosic biomass. *Bioresource Technology 100*, 10–18.

Vogel, J. (2008) Unique aspects of the grass cell wall. *Current Opinion in Plant Biology 11*, 301–307.

Dhepe, P. L., and Sahu, R. (2010) A solid-acid-based process for the conversion of hemicellulose. *Green Chemistry 12*, 2153–2156.

Saha, B. C. (2003) Hemicellulose bioconversion. *Journal of Industrial Microbiology and Biotechnology 30*, 279–291.

Lora, J. In *Monomers, Polymers and Composites from Renewable Resources*; Belgacem, M. N., and Gandini, A., Eds.; Elsevier: Amsterdam, 2008; pp 225–241.

Ten, E., and Vermerris, W. (2015) Recent developments in polymers derived from industrial lignin. *Journal of Applied Polymer Science 132*.

Kautto, J., Realff, M. J., Ragauskas, A. J., and Kässi, T. (2014) Economic Analysis of an Organosolv Process for Bioethanol Production. *BioRes 9*, 6041–6072.

Wild, P. J. D., Huijgen, W. J. J., and Gosselink, R. J. (2014) Lignin pyrolysis for profitable lignocellulosic biorefineries. *Biofuels, Bioproducts and Biorefining 8*, 645–657.

Kumar, P., Barrett, D. M., Delwiche, M. J., and Stroeve, P. (2009) Methods for Pretreatment of Lignocellulosic Biomass for Efficient Hydrolysis and Biofuel Production. *Industrial & Engineering Chemistry Research 48*, 3713–3729.

Brodin, M., Vallejos, M., Opedal, M. T., Area, M. C., and Chinga-Carrasco, G. (2017) Lignocellulosics as sustainable resources for production of bioplastics – A review. *Journal of Cleaner Production 162*, 646–664.

Jacquet, N., Maniet, G., Vanderghem, C., Delvigne, F., and Richel, A. (2015) Application of Steam Explosion as Pretreatment on Lignocellulosic Material: A Review. *Industrial & Engineering Chemistry Research 54*, 2593–2598.

Schutyser, W., Renders, T., Van den Bosch, S., Koelewijn, S.-F., Beckham, G. T., and Sels, B. F. (2018) Chemicals from lignin: an interplay of lignocellulose fractionation, depolymerisation, and upgrading. *Chemical Society Reviews 47*, 852–908.

Bajwa, D., Pourhashem, G., Ullah, A., and Bajwa, S. (2019) A concise review of current lignin production, applications, products and their environmental impact. *Industrial Crops and Products 139*, 111526.

Ahvazi, B., Cloutier, E., Wojciechowicz, O., and Ngo, T.-D. (2016) Lignin Profiling: A Guide for Selecting Appropriate Lignins as Precursors in Biomaterials Development. *ACS Sustainable Chemistry & Engineering 4*, 5090–5105.

Mandlekar, N., Cayla, A., Rault, F., Giraud, S., Salaün, F., Malucelli, G., and Guan, J.-P. *Lignin - Trends and Applications*; InTech, 2018.

Pan, X., Kadla, J. F., Ehara, K., Gilkes, N., and Saddler, J. N. (2006) Organosolv Ethanol Lignin from Hybrid Poplar as a Radical Scavenger: Relationship between Lignin Structure, Extraction Conditions, and Antioxidant Activity. *Journal of Agricultural and Food Chemistry 54*, 5806–5813.

Pinheiro, F. G. C., Soares, A. K. L., Santaella, S. T., Silva, L. M. A. e., Canuto, K. M., Cáceres, C. A., Rosa, M. d. F., Feitosa, J. P. d. A., and Leitão, R. C. (2017) Optimization of the acetosolv extraction of lignin from sugarcane bagasse for phenolic resin production. *Industrial Crops and Products 96*, 80–90.

Zijlstra, D. S., Analbers, C. A., de Korte, J., Wilbers, E., and Deuss, P. J. (2019) Efficient Mild Organosolv Lignin Extraction in a Flow-Through Setup Yielding Lignin with High β-O-4$'$Content. *Polymers 11*, 1913.

Li, M.-F., Sun, S.-N., Xu, F., and Sun, R.-C. (2012) Formic acid based organosolv pulping of bamboo (Phyllostachys acuta): Comparative characterization of the dissolved lignins with milled wood lignin. *Chemical Engineering Journal 179*, 80–89.

Teng, J., Ma, H., Wang, F., Wang, L., and Li, X. (2016) Catalytic Fractionation of Raw Biomass to Biochemicals and Organosolv Lignin in a Methyl Isobutyl Ketone/H2O Biphasic System. *ACS Sustainable Chemistry & Engineering 4*, 2020–2026.

Shuai, L., Questell-Santiago, Y. M., and Luterbacher, J. S. (2016) A mild biomass pretreatment using γ-valerolactone for concentrated sugar production. *Green Chemistry 18*, 937–943.

Ragauskas, A. J. et al. (2014) Lignin Valorization: Improving Lignin Processing in the Biorefinery. *American Association for the Advancement of Science 344*, 1246843–1246843.

Xu, J., Li, C., Dai, L., Xu, C., Zhong, Y., Yu, F., and Si, C. (2020) Biomass Fractionation and Lignin Fractionation towards Lignin Valorization. *ChemSusChem 13*, 4284–4295.

Vila, C., Santos, V., and Parajó, J. C. (2003) Simulation of an Organosolv Pulping Process: Generalized Material Balances and Design Calculations. *Industrial & Engineering Chemistry Research 42*, 349–356.

Kautto, J., Realff, M. J., Ragauskas, A. J., and Kässi, T. (2014) Economic Analysis of an Organosolv Process for Bioethanol Production. *BioResources 9*, 6041–6072.

Budzinski, M., and Nitzsche, R. (2016) Comparative economic and environmental assessment of four beech wood based biorefinery concepts. *Bioresource Technology 216*, 613–621.

Li, M.-F., Sun, S.-N., Xu, F., and Sun, R.-C. (2012) Mild Acetosolv Process To Fractionate Bamboo for the Biorefinery: Structural and Antioxidant Properties of the Dissolved Lignin. *Journal of Agricultural and Food Chemistry 60*, 1703–1712.

Ligero, P., Vega, A., and Bao, M. (2005) Acetosolv delignification of Miscanthus sinensis bark. *Industrial Crops and Products 21*, 235–240.

Ligero, P., Villaverde, J. J., de Vega, A., and Bao, M. (2008) Delignification of Eucalyptus globulus saplings in two organosolv systems (formic and acetic acid). *Industrial Crops and Products 27*, 110–117.

Boerjan, W., Ralph, J., and Baucher, M. (2003) Lignin Biosynthesis. *Annual Review of Plant Biology 54*, 519–546.

Vanholme, R., Demedts, B., Morreel, K., Ralph, J., and Boerjan, W. (2010) Lignin Biosynthesis and Structure. *Plant Physiology 153*, 895–905.

Vanholme, R., De Meester, B., Ralph, J., and Boerjan, W. (2019) Lignin biosynthesis and its integration into metabolism. *Current Opinion in Biotechnology 56*, 230–239.

Ma, R., Guo, M., and Zhang, X. *Lignin Valorization: Emerging Approaches*; The Royal Society of Chemistry, 2018; pp 128–158.

Vanholme, R., Morreel, K., Ralph, J., and Boerjan, W. (2008) Lignin engineering. *Current Opinion in Plant Biology 11*, 278–285.

Guadix-Montero, S., and Sankar, M. (2018) Review on Catalytic Cleavage of C–C Inter-unit Linkages in Lignin Model Compounds: Towards Lignin Depolymerisation. *Topics in Catalysis 61*, 183–198.

Karlen, S. D. et al. (2016) Monolignol ferulate conjugates are naturally incorporated into plant lignins. *Science Advances 2*.

Buranov, A. U., and Mazza, G. (2008) Lignin in straw of herbaceous crops. *Industrial Crops and Products 28*, 237–259.

Min, D.-y., Chang, H.-m., Jameel, H., Lucia, L., Wang, Z.-g., and Jin, Y.-c. (2014) The Structure of Lignin of Corn Stover and its Changes Induced by Mild Sodium Hydroxide Treatment. *BioResources 9*, 2405–2414.

Grand View Research, *Lignin Market Size, Share & Trends Analysis Report By Product (Ligno-Sulphonates, Kraft, Organosolv), By Application (Macromolecule, Aromatic), By Region, And Segment Forecasts, 2020 - 2027*; 2020.

Silverman, J. R., Danby, A. M., and Subramaniam, B. (2020) Facile Prepolymer Formation with Ozone-Pretreated Grass Lignin by In Situ Grafting of Endogenous Aromatics. *ACS Sustainable Chemistry & Engineering 8*, 17001–17007.

Gandini, A., and Belgacem, M. N. In *Monomers, Polymers and Composites from Renewable Resources*; Belgacem, M. N., and Gandini, A., Eds.; Elsevier: Amsterdam, 2008; pp 243–271.

Sun, Z., Fridrich, B., de Santi, A., Elangovan, S., and Barta, K. (2018) Bright Side of Lignin Depolymerization: Toward New Platform Chemicals. *Chemical Reviews 118*, 614–678, PMID: 29337543.

Zabkova, M., da Silva, E. B., and Rodrigues, A. (2007) Recovery of vanillin from Kraft lignin oxidation by ion-exchange with neutralization. *Separation and Purification Technology 55*, 56–68.

Walton, N. J., Mayer, M. J., and Narbad, A. (2003) Molecules of Interest: Vanillin. *Phytochemistry 63*, 505–515.

Van den Bosch, S., Koelewijn, S.-F., Renders, T., Van den Bossche, G., Vangeel, T., Schutyser, W., and Sels, B. F. (2018) Catalytic Strategies Towards Lignin-Derived Chemicals. *Topics in Current Chemistry 376*.

Reports,, and Data, *Vanillin Market Analysis, By Type (Natural, Synthetic), By Sales Channel (Online Selling, Offline Selling), By End-Use Verticals (Food & Beverage, Cosmetics & Toiletries, Therapeutic Treatment, Pharmaceuticals), Forecasts To 2027*; 2020; p 287.

Imre, B., and Pukánszky, B. (2015) From natural resources to functional polymeric biomaterials. *European Polymer Journal 68*, 481–487.

Amarasekara, A. S., Wiredu, B., and Razzaq, A. (2012) Vanillin based polymers: I. An electrochemical route to polyvanillin. *Green Chemistry 14*, 2395.

Abu-Omar, M. M., Barta, K., Beckham, G. T., Luterbacher, J. S., Ralph, J., Rinaldi, R., Román-Leshkov, Y., Samec, J. S. M., Sels, B. F., and Wang, F. (2021) Guidelines for performing lignin-first biorefining. *Energy & Environmental Science 14*, 262–292.

Ma, R., Guo, M., and Zhang, X. (2018) Recent advances in oxidative valorization of lignin. *Catalysis Today 302*, 50–60.

Banu, J. R., Kavitha, S., Yukesh Kannah, R., Poornima Devi, T., Gunasekaran, M., Kim, S.-H., and Kumar, G. (2019) A review on biopolymer production via lignin valorization. *Bioresource Technology 290*, 121790.

Li, C., Zhao, X., Wang, A., Huber, G. W., and Zhang, T. (2015) Catalytic Transformation of Lignin for the Production of Chemicals and Fuels. *Chemical Reviews 115*, 11559–11624.

Cheng, C., Wang, J., Shen, D., Xue, J., Guan, S., Gu, S., and Luo, K. (2017) Catalytic Oxidation of Lignin in Solvent Systems for Production of Renewable Chemicals: A Review. *Polymers 9*, 240.

Liu, X., Bouxin, F. P., Fan, J., Budarin, V. L., Hu, C., and Clark, J. H. (2020) Recent Advances in the Catalytic Depolymerization of Lignin towards Phenolic Chemicals: A Review. *ChemSusChem 13*, 4296–4317.

Tarabanko, V. E., Petukhov, D. V., and Selyutin, G. E. (2004) New Mechanism for the Catalytic Oxidation of Lignin to Vanillin. *Kinetics and Catalysis 45*, 569–577.

Nandiwale, K. Y., Danby, A. M., Ramanathan, A., Chaudhari, R. V., and Subramaniam, B. (2017) Zirconium-Incorporated Mesoporous Silicates Show Remarkable Lignin Depolymerization Activity. *ACS Sustainable Chemistry & Engineering 5*, 7155–7164.

Nandiwale, K. Y., Danby, A. M., Ramanathan, A., Chaudhari, R. V., and Subramaniam, B. (2019) Dual Function Lewis Acid Catalyzed Depolymerization of Industrial Corn Stover Lignin into Stable Monomeric Phenols. *ACS Sustainable Chemistry & Engineering 7*, 1362–1371.

Dai, J., Patti, A. F., and Saito, K. (2016) Recent developments in chemical degradation of lignin: catalytic oxidation and ionic liquids. *Tetrahedron Letters 57*, 4945–4951.

Chatel, G., and Rogers, R. D. (2014) Review: Oxidation of Lignin Using Ionic Liquids—An Innovative Strategy To Produce Renewable Chemicals. *ACS Sustainable Chemistry & Engineering 2*, 322–339.

Danby, A. M., Lundin, M. D., and Subramaniam, B. (2018) Valorization of Grass Lignins: Swift and Selective Recovery of Pendant Aromatic Groups with Ozone. *ACS Sustainable Chemistry & Engineering 6*, 71–76.

Silverman, J. R., Danby, A. M., and Subramaniam, B. (2019) Intensified ozonolysis of lignins in a spray reactor: insights into product yields and lignin structure. *React. Chem. Eng. 4*, 1421–1430.

Song, Q., Wang, F., Cai, J., Wang, Y., Zhang, J., Yu, W., and Xu, J. (2013) Lignin depolymerization (LDP) in alcohol over nickel-based catalysts via a fragmentation–hydrogenolysis process. *Energy & Environmental Science 6*, 994.

Houfani, A. A., Anders, N., Spiess, A. C., Baldrian, P., and Benallaoua, S. (2020) Insights from enzymatic degradation of cellulose and hemicellulose to fermentable sugars– a review. *Biomass and Bioenergy 134*, 105481.

Janusz, G., Pawlik, A., Sulej, J., Świderska Burek, U., Jarosz-Wilkołazka, A., and Paszczyński, A. (2017) Lignin degradation: microorganisms, enzymes involved, genomes analysis and evolution. *FEMS Microbiology Reviews 41*, 941–962.

Wen, X., Jia, Y., and Li, J. (2009) Degradation of tetracycline and oxytetracycline by crude lignin peroxidase prepared from Phanerochaete chrysosporium–a white rot fungus. *Chemosphere 75*, 1003—1007.

Shinners, K. J., and Binversie, B. N. (2007) Fractional yield and moisture of corn stover biomass produced in the Northern US Corn Belt. *Biomass and Bioenergy 31*, 576–584.

Blandino, M., Fabbri, C., Soldano, M., Ferrero, C., and Reyneri, A. (2016) The use of cobs, a by-

product of maize grain, for energy production in anaerobic digestion. *Italian Journal of Agronomy 11*, 195.

NASS, *Corn Production*; National Agricultural Statistics Service (NASS) at the United States Department of Agriculture, 2021.

NASS, *2019 State Agriculture Overview*; National Agricultural Statistics Service (NASS) at the United States Department of Agriculture, 2019.

Pordesimo, L. O., Edens, W. C., and Sokhansanj, S. Distribution of Above Ground Biomass in Corn Stover. ASABE Paper No. 026059. 2002.

Birrell, S. J., Karlen, D. L., and Wirt, A. (2014) Development of Sustainable Corn Stover Harvest Strategies for Cellulosic Ethanol Production. *BioEnergy Research 7*, 509–516.

Liao, Y. et al. (2020) A sustainable wood biorefinery for low–carbon footprint chemicals production. *Science 367*, 1385–1390.

Kangas, H., Liitiä, T., Rovio, S., Ohra-aho, T., Heikkinen, H., Tamminen, T., and Poppius-Levlin, K. (2015) Characterization of dissolved lignins from acetic acid Lignofibre (LGF) organosolv pulping and discussion of its delignification mechanisms. *Holzforschung 69*, 247–256.

Binder, T., and Hagberg, E. Delivered in closed project meeting.

Woźniak, M., Ratajczak, I., Wojcieszak, D., Waśkiewicz, A., Szentner, K., Przybył, J., Borysiak, S., and Goliński, P. (2021) Chemical and Structural Characterization of Maize Stover Fractions in Aspect of Its Possible Applications. *Materials 14*, 1527.

Wen, J.-L., Xue, B.-L., Xu, F., and Sun, R.-C. (2012) Unveiling the Structural Heterogeneity of Bamboo Lignin by In Situ HSQC NMR Technique. *BioEnergy Research 5*, 886–903.

Timokhin, V. I., Regner, M., Motagamwala, A. H., Sener, C., Karlen, S. D., Dumesic, J. A., and Ralph, J. (2020) Production of p-Coumaric Acid from Corn GVL-Lignin. *ACS Sustainable Chemistry & Engineering 8*, 17427–17438.

Schiaffo, C. E., and Dussault, P. H. (2008) Ozonolysis in Solvent/Water Mixtures: Direct Conversion of Alkenes to Aldehydes and Ketones. *The Journal of Organic Chemistry 73*, 4688–4690.

Cerruto, E., Manetto, G., Papa, R., and Longo, D. (2021) Modelling Spray Pressure Effects on Droplet Size Distribution from Agricultural Nozzles. *Applied Sciences 11*, 9283.

Novo, L. P., and Curvelo, A. A. S. (2019) Hansen Solubility Parameters: A Tool for Solvent Selection for Organosolv Delignification. *Industrial & Engineering Chemistry Research 58*, 14520–14527.

Seem, T. C., Rowson, N. A., Ingram, A., Huang, Z., Yu, S., de Matas, M., Gabbott, I., and Reynolds, G. K. (2015) Twin screw granulation — A literature review. *Powder Technology 276*, 89–102.

Kinn, B. Separation and Purification of Vanillin and *p*-Hydroxybenzaldehyde from Grass Lignins. M.Sc. thesis, University of Kansas, 2022; Submitted.

Subramaniam, B., Rajewski, R. A., and Bochniak, D. J. Process and Apparatus for Size Selective Separation of Micro- and Nano-Particles. 2000.

Snavely, W. K., Subramaniam, B., Rajewski, R. A., and Defelippis, M. R. (2002) Micronization of insulin from halogenated alcohol solution using supercritical carbon dioxide as an antisolvent. *Journal of Pharmaceutical Sciences 91*, 2026–2039.

Appendix A

Supplementary Information

A.1 Abbreviations

Abbr.	Definition	Abbr.	Definition
AcOH	acetic acid	HSQC	heteronuclear single quantum coherence
ADM	Archer Daniels Midland Company	ICP	inductively coupled plasma
CHNO	carbon, hydrogen, nitrogen, oxygen	IL	ionic liquid
CL	corn cob lignin	LCC	lignin-carbohydrate complex
DMF	dimethylformamide	LFCC	lignin-ferulate-carbohydrate complex
EtAC	ethyl acetate	LMW	low molecular weight fraction
FID	flame ionization detector	LPR	liquid-phase reforming
FmOH	formic acid	NMR	nuclear magnetic resonance
FTIR	fourier-transform infrared	OZCL	ozonized corn cob lignin
GC	gas chromatography	*p*HB	*p*-hydroxybenzaldehyde
GPC	gel-permeation chromatography	PF	phenol-formaldehyde resin
GVL	γ-valerolactone	RCF	reductive catalytic fractionation
H/G/S	hydroxyphenyl, guaiacyl, syringyl	SAS	supercritical antisolvent
HMW	high molecular weight fraction	SL	corn stover lignin

A.2 Materials

A.2.1 Acetosolv Extraction

Initial samples of corn stover (SL3) and corn cobs (CL3) were collected from a local field in Lawrence, Kansas. Subsequent extractions (CL2 and other unpublished samples) were performed on corn cobs supplied by J-SIX Enterprises, a corn cob processing plant in Seneca, Kansas. All solvents, glacial acetic acid, sulfuric acid, reagent ethanol (5% methanol and 5% isopropanol), and

DMSO-d6 were purchased from TCI America.

A.2.2 Spray Ozonolysis

Glacial acetic acid, formic acid (88%), γ-valerolactone, and methanol (HPLC grade) were purchased from TCI America. Three lignin samples (SL1, SL2, and CL1) were provided by ADM. The remaining lignin samples (SL3, CL2, CL3, and other unpublished samples) were extracted using the method described in Chapter 2. Compounds used for GC/FID calibration and identification (vanillin, *p*HB, vanillic acid, *p*-hydroxybenzoic acid) were purchased from Sigma Aldrich. Powdered KBr for FTIR was also purchased from Sigma Aldrich.

A.3 Experimental Methods

A.3.1 Spray Ozonolysis of Lignin

The normally solid lignin must be dissolved in a suitable protic solvent for spraying. A typical experiment used a glacial acetic acid and 88% formic acid mixture at 3:1 v/v. The final ratio of acetic to formic to water was 75:22:3 by volume. In a preliminary solvent experiment, the ratio was modified or singular mixtures of aqueous acetic acid or aqueous formic acid were used. In all experiments, the lignin was completely solubilized to a concentration of 1.0 wt.%.

Prior to every experiment, the ozone generator was allowed to warm up and purge the reactor. The ozone concentration at the inlet and outlet were equilibrated at experimental conditions (1-5 mol.% O_3) before any experiment could begin. A rotameter was used to control the gas flow rate to 1.0-4.0 SLPM. Once equilibrated, the lignin solution is pumped into the chamber through an MW085 Bete MicroWhirl spray nozzle. A syringe pump maintains a constant flow rate of 3-7 LPH, depending upon the experiment.

Inside the chamber, lignin exits the nozzle at ca. 400 psi where it instantaneously atomizes into a conical plume of small drops. During a brief residence of 5-8 s, the lignin spray collides counter-current to the stream of ozone such that the contact time is minimized. The droplets then

coalesce and exit through the bottom valve to be sampled and analyzed. The collected mixture contains the phenolic aldehyde products and the remaining ozonized lignin.

A.3.2 Gas Chromatography/Flame Ionization Detector (GC/FID) & /Mass Spectroscopy (GC/MS)

Lignin samples before and after ozonolysis were analyzed and quantified with GC/FID using an Agilent 7890A GC and HP-INNOWAX column. Samples were diluted by combining 300 µL of lignin solution with 1.0 mL of methanol. Prior to dilution, samples were filtered using a 0.2 µm syringe filter. The parameters for GC analysis were as follows: 1 µL injection volume, inlet temperature of 250 °C, 2 SCCM of helium carrier gas, and initial oven temperature of 40 °C. The initial oven temperature was held constant for 5 min followed by a ramp of 10 °C/min to 220 °C where it then remained for another 20 min. Quantification relied upon calibration curves using external standards of concentrations that were expected in the experimental samples. Calibration curves for *p*-hydroxybenzaldehyde and vanillin can be seen in Figures A.1a and A.1b. For peak identification purposes, standard solutions were analyzed and their retention times were cataloged. GC/MS was also used in molecular identification using an identical method and column as described for GC/FID. An Agilent 5975C MS scanned masses from 20 to 500 Da.

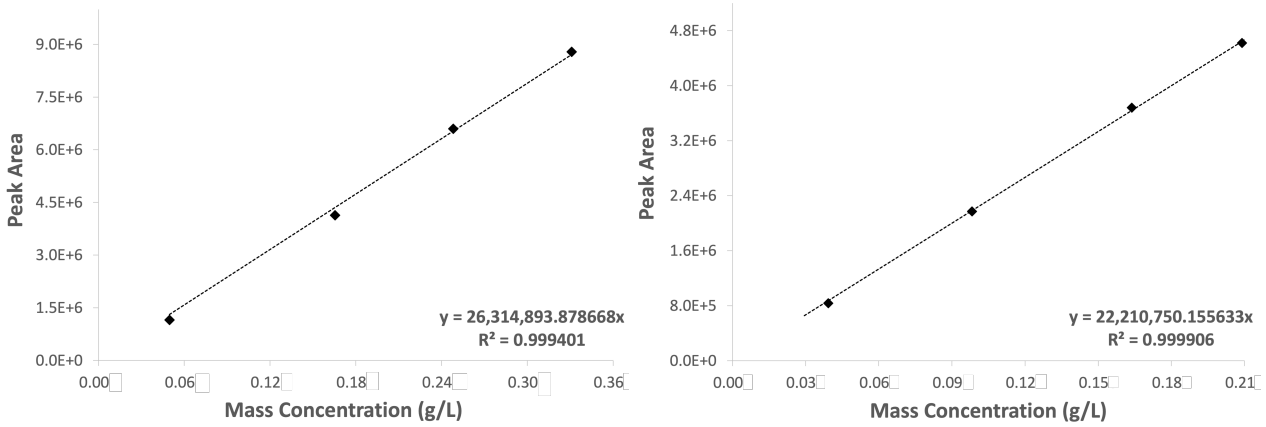

(a) *p*-hydroxybenzaldehyde (b) vanillin

Figure A.1: External calibration curves for GC/FID quantification using purchased standards.

A.3.3 Heteronuclear Single Quantum Coherence (HSQC) NMR

Nuclear magnetic resonance (NMR) spectra of lignin samples were acquired in a Bruker AVIII 500 MHz spectrometer with a multinuclear BFFO cryoprobe. Two-dimensional ^{1}H-^{13}C HSQC spectra were obtained with a standard hsqcedetgpsisp2.2 pulse sequence. A typical experiment used the following parameters: 16 scans, 2 second relaxation delay, 256 time increments in the ^{13}C dimension, and spectral widths of 10 ppm for ^{1}H dimension and 210 ppm for ^{13}C dimension. Samples were prepared by dissolving approximately 75 mg of lignin, ozonized lignin, or compound standard with 0.75 mL of dimethylsulfoxide-d_6 (DMSO-d_6). Analytical spectral processing was carried out using MestreNova software. Chemical shift calibration was performed using the central DMSO-d_6 peak ($\delta H/\delta C$ 39.5/2.50).

A.3.4 Fourier Transform Infrared Spectroscopy (FTIR)

FTIR absorption spectra were obtained using a Bruker Tensor T27 FTIR. Spectra were collected using 64 scans over the range of 400 to 4000 cm^{-1}. Background spectra were collected then removed from sample spectra. Samples were prepared by combining ca. 5 mg of lignin sample with KBr powder then pressing the finely mixed powder into a disc. Peaks were identified using reported findings from other literature.

A.3.5 Gel-Permeation Chromatography (GPC)

GPC analysis was performed on an Agilent 1260 Infiniti GPC system. Analyte signal was detected by an Agilent refractive index detector after passing through a 300 mm Polargel-M and a 300 mm Polargel-L in series. While holding the columns at 40 °C, samples were eluted with 1.0 mL/min of the mobile phase (non-gradient). The mobile phase was dimethylformamide stabilized with 0.1 wt.% of tetrabutyl-ammonium bromide. Chromatograms were calibrated against poly(methyl methacrylate) standards. Samples were prepared by evaporating the solvent to recovered approximately 40 mg of sample and redissolving in 1.0 mL of the mobile phase.

A.3.6 CHNO Elemental Analysis

Elemental analysis was conducted by contracted services provided by Archer Daniels Midland Company (ADM) and Midwest Microlab. Composition of CHN was measured by a single CHN analyzing instrument. Extractives composition was measured by an Inductively Coupled Plasma (ICP) instrument. ICP is capable of detecting elements larger than sodium (Na). O% was calculated as the remainder of 100% less the composition of C%, H%, N% and detected extractives.

A.4 Experimental Data

A.4.1 Blank Runs of Pure Solvent Sprayed into Ozone

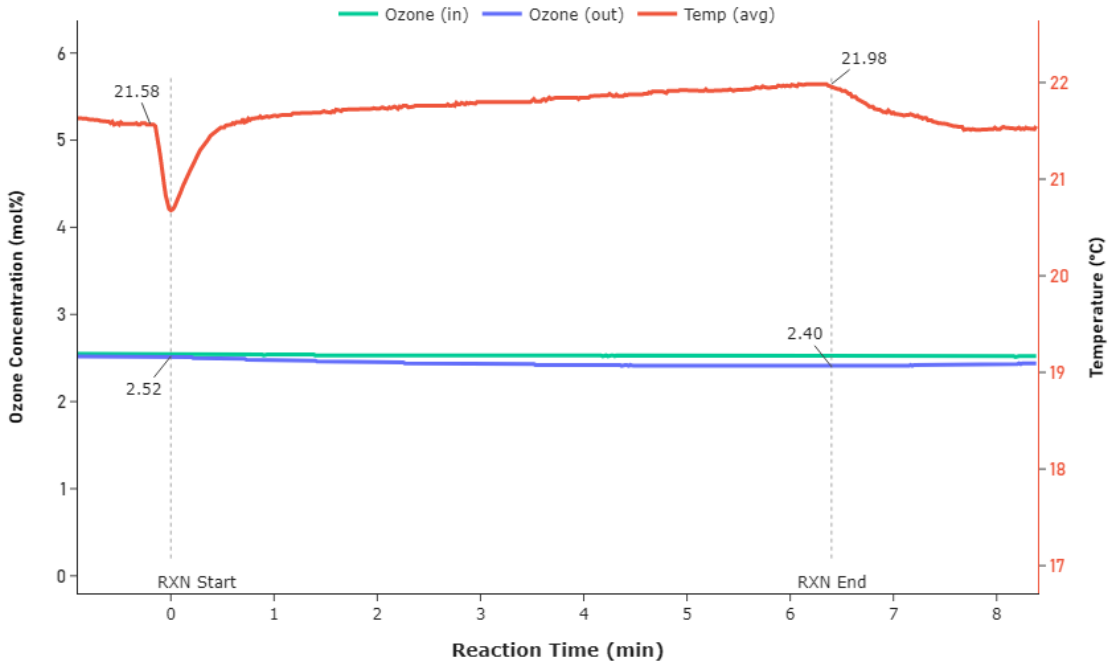

Figure A.2: Temporal temperature and ozone concentration profiles for spray ozonolysis experiment consisting of only **3:1 v/v AcOH:FmOH solution**.

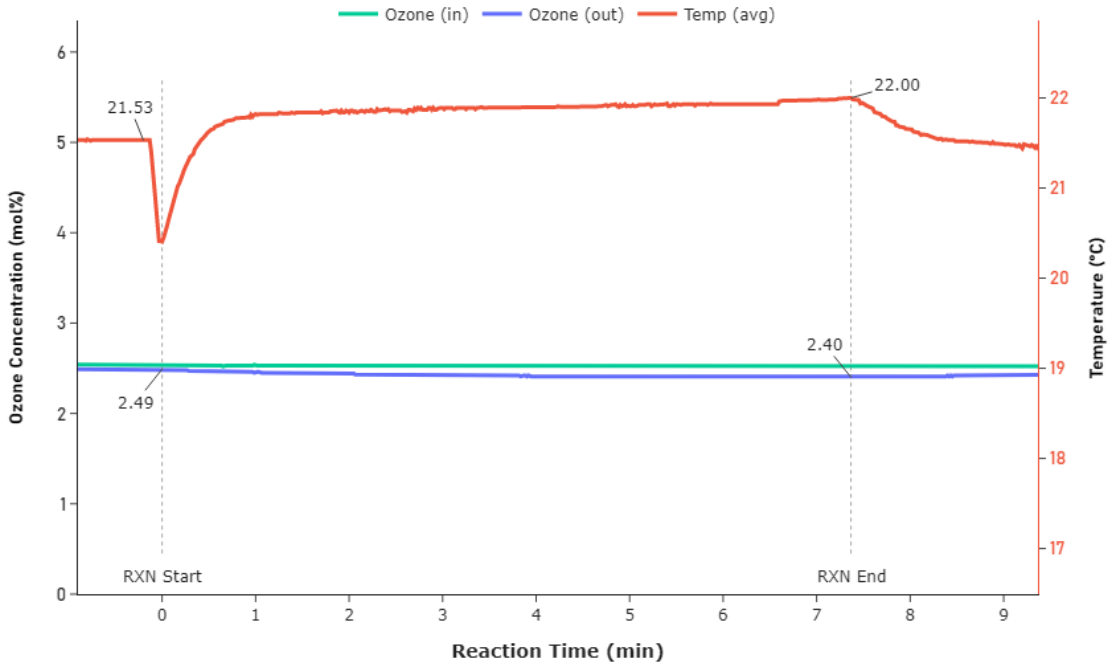

Figure A.3: Temporal temperature and ozone concentration profiles for spray ozonolysis experiment consisting of only **88% acetic acid**.

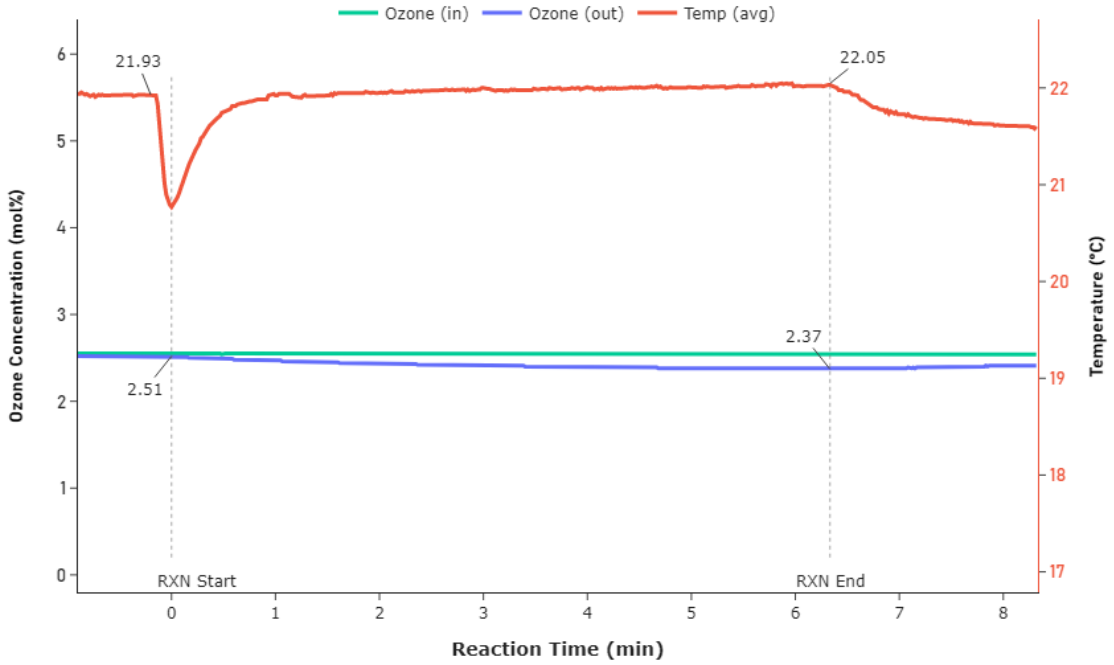

Figure A.4: Temporal temperature and ozone concentration profiles for spray ozonolysis experiment consisting of only **88% formic acid**.

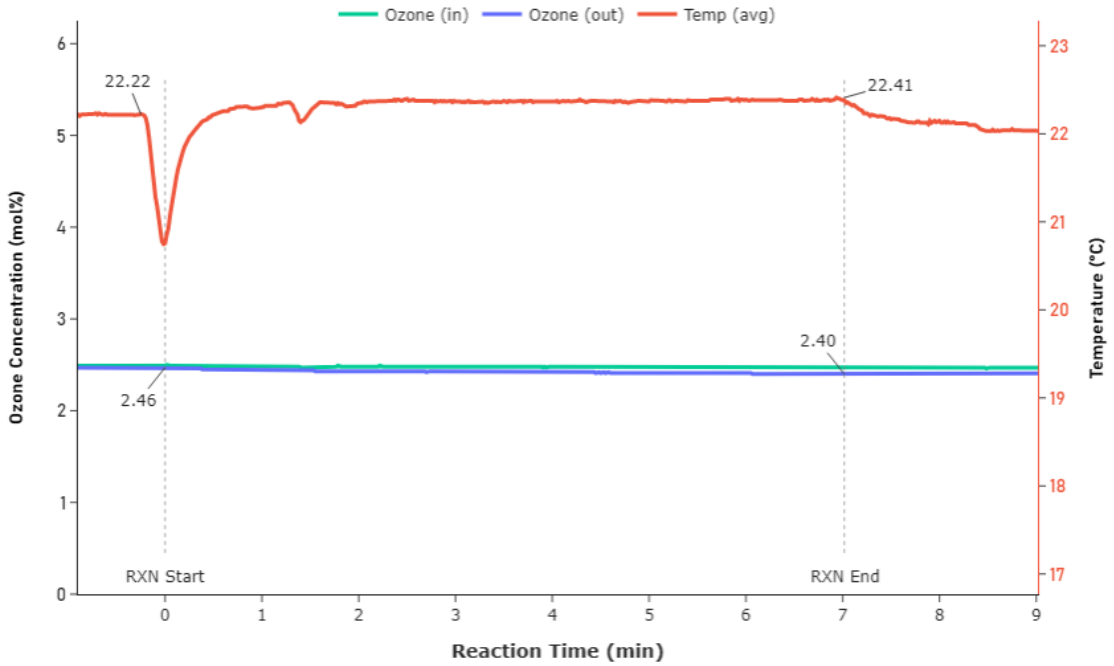

Figure A.5: Temporal temperature and ozone concentration profiles for spray ozonolysis experiment consisting of only **water**.

A.5 Process and Equipment Photographs

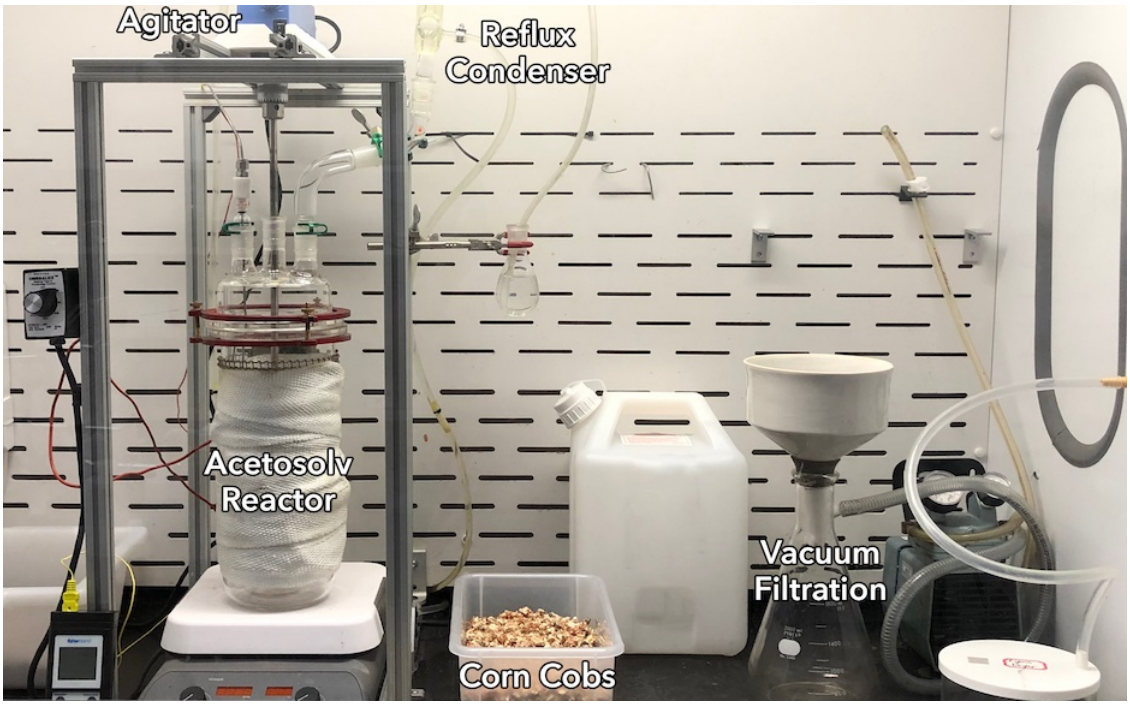

Figure A.6: Photo of acetosolv extraction setup including 4 L reactor with mixer and vacuum filtration.

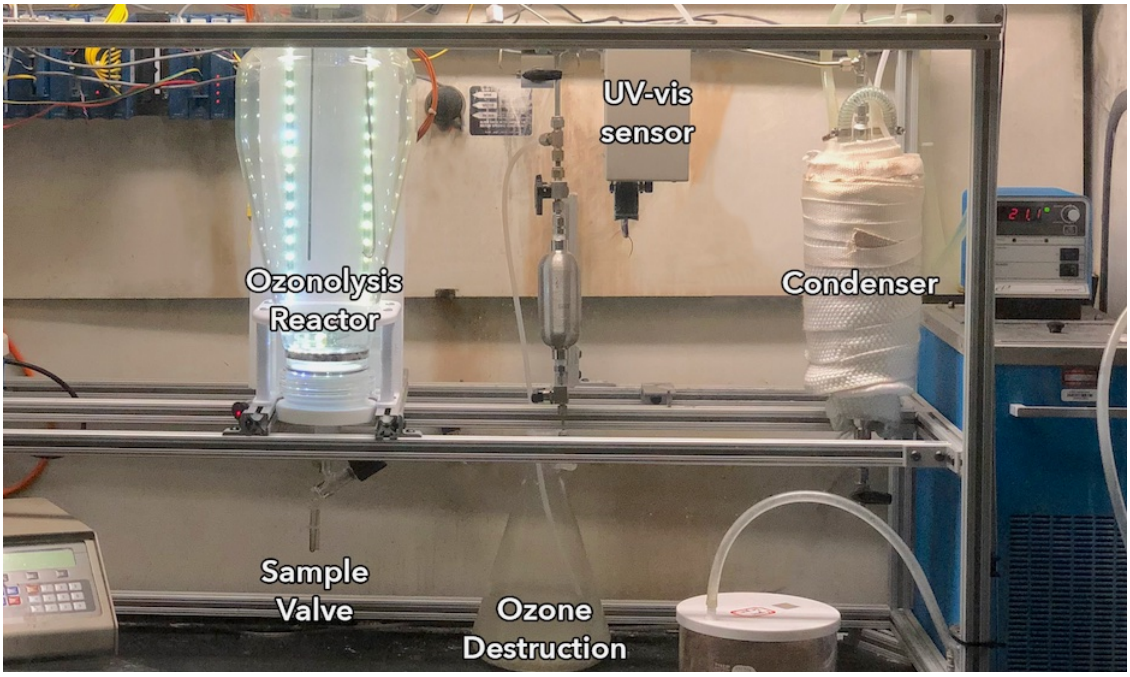

Figure A.7: Photo of spray ozonolysis setup including 6 L ozonolysis reactor and entrained vapor condenser.

A.6 Calculations for Elemental Analysis of Ozonized Cob Lignin

$$\frac{1mol\ C=C}{1mol\ ph.ald.} * \frac{1mol\ O_2}{1mol\ C=C} * \frac{32g}{1mol\ O_2} = \frac{32g\ O_2}{molph.ald.} \tag{A.1}$$

$$\frac{7.50g\ coum.\ +\ 2.50g\ ferul.}{100g\ lignin} * \frac{1mol\ ph.ald.}{164.05g\ +\ 194.18g} * \frac{32g\ O_2}{molph.ald.} = 1.72g\ O_2 \tag{A.2}$$